8987-0001-RU-000

FINAL REPORT
CHARGED PARTICLE RADIATION DAMAGE IN SEMICONDUCTORS, I: EXPERIMENTAL PROTON IRRADIATION OF SOLAR CELLS

Contract No. NAS 5-613

15 September 1961

SPACE TECHNOLOGY LABORATORIES, INC.
P. O. Box 95001
Los Angeles 45, California

ERRATA SHEET

1. Throughout this report the term "oxygen-free silicon" refers to silicon produced by the float-zone process. The oxygen content of float-zone silicon is usually 100 to 1000 times lower than the oxygen content of grown silicon crystals. However, in none of the specimens described in this report was an actual oxygen concentration determination made after diffusing to form the junction.

2. Refer to Figure 10, Page 24: The curves in this figure should be labeled 1 through 4 in descending order. For example, Curve 1 has the highest spectral response.

CHARGED PARTICLE RADIATION DAMAGE IN SEMICONDUCTORS, I: EXPERIMENTAL PROTON IRRADIATION OF SOLAR CELLS

Prepared by: J. M. Denney

Prepared by: R. G. Downing

ABSTRACT

The effect of proton bombardment on solar cells, particularly silicon, has been experimentally measured at proton energies from 20.5 Mev to 740 Mev. Comparison of cell type, cell geometry, and parent material, as well as current-voltage characteristics, spectral response, and current decay, with integrated flux at four proton energies is presented. It is found that a relation of the form

$$I_{sc} = I_{sc_o} \left[I - k(\lambda) \log (\Phi / \Phi_k) \right]$$

describes the loss of output of all solar cells under proton bombardment in this energy range. The radiation resistance of shallow diffused oxygen-free p on n silicon cells exceeds conventional cells by a factor of at least five and exceeds n on p cells by a small percentage. The control of radiation resistance by oxygen and other factors is discussed, and the observation of annealing in n on p cells at room temperature is noted. Curves summarizing radiation damage rates, for power supply design, are presented.

TABLE OF CONTENTS

ACKNOWLEDGEMENT

We are grateful to a host of individuals for their assistance and encouragement. Professor R. C. Thornton and Mr. J. Vale, University of California, Lawrence Radiation Laboratory; Dr. S. C. Wright, Fermi Institute, University of Chicago; Professor J. Richardson, University of California at Los Angeles; Mr. W. Cherry, U. S. Army Signal Research and Development Laboratory; Dr. B. Ross, Hoffman Semiconductor; Dr. L. DeVore, Hoffman Research Center; Dr. M. Wolff, Heliotek; Mr. P. Rappaport, RCA; Dr. W. Brown, Mr. F. Smits, and Dr. W. Rosensweig, Bell Telephone Laboratories; Dr. W. Cooley and Mr. H. Talkin, NASA; Professor G. Pearson, Stanford University; Dr. N. Snyder, Institute for Defense Analysis. The California and University of Chicago experiments and analysis were supported by the National Aeronautics and Space Administration, Contract NAS 5-613.

LIST OF ILLUSTRATIONS

1.0 INTRODUCTION

In recent years, the growing knowledge of bands of charged particles surrounding the earth has increased attention to radiation damage in spacecraft components and materials. High energy protons in the inner Van Allen belt have increased interest in measuring the effects produced by proton bombardment. Solar cells are convenient research tools and important spacecraft components. Also, because solar cells are generally more sensitive to radiation damage than other semiconductor components, they warrant additional attention.

This study compares the effects of proton bombardment of solar cells observed in many experiments at proton energies of 740 Mev, 450 Mev, 400 Mev, and 20.5 Mev. Comparison of a variety of solar cells at each energy is included in order to study the effects of solar cell characteristics on radiation resistance.

2.0 DESCRIPTION OF EXPERIMENTS

A number of cyclotrons have been employed in the experimental study of radiation damage in solar cells. Despite the general similarities of cyclotrons, each machine has unique characteristics which require individual attention to experiment design. In this section, the experimental methods are presented separately for each cyclotron in reasonably complete detail, in the interest of clarity and at the expense of redundancy.

2.1 740 Mev Experiments

These experiments were conducted at the 184-inch synchrocyclotron at the Lawrence Radiation Laboratory, University of California. The external proton beam current was about 2×10^{-8} amperes. The defocused beam covered an area of about four square inches at the exit port with intensity uniform within 20 per cent. The total beam current was measured by a secondary emission monitor[1] which had been previously calibrated at low beam currents by simultaneous comparison with an argon filled ionization chamber. The ionization chamber was calibrated by both absolute count rate measurements and proton scattering experiments. The secondary emission monitor output was found to be linear with beam current and indicated total beam current with an accuracy of 5 per cent. The total beam current in all experiments was measured, time integrated, and recorded with an integrating electrometer and strip chart recorder. The accuracy of the time integrated beam current was found to be 5 per cent, limited by the secondary emission monitor accuracy.

The relative proton intensity, specimen alignment in the beam, and beam shape were determined by exposure of x-ray films. Densitometric analysis of the x-ray films determined the proton flux on the specimens. X-ray films exposed in the specimen holder at intervals during the experiments were developed under carefully controlled conditions. The optical transmission of these developed films as a function of position was measured with a film densitometer. The proportionality between the measured film density and proton intensity was obtained using H and D curves for the film and establishing that the density in the developed film did

---

[1] G. W. Tautfest and H. R. Fechter, Review Scientific Instrumentation, 26, 299, (1955)

characteristics with an X-Y plotter, Figure 1. A series of calibrated solar cells were used to maintain the relative light intensity at the illumination plane to within ± 2 per cent. The absolute value of energy at the illumination plane was approximately 80 mw/cm^2 equivalent sunlight as seen by a standard p on n silicon solar cell. Due to the difference in spectral content of tungsten light and sunlight, this equivalent energy will vary depending on the spectral response characteristics of the individual solar cells. Therefore, no effort was extended to accurately determine the absolute value of the energy at the illumination plane; rather the relative value of energy throughout the course of the measurements was maintained constant by the use of the calibrated solar cells.

Unfiltered 2800°K tungsten light for I-V characteristics was chosen for experimental convenience. The use of tungsten illumination does not compromise the value of the experimental results provided the absolute spectral response is also measured. Spectral response of all irradiated cells was determined both before and after irradiation. Because radiation damage in silicon solar cells produces a greater change in output for the red component of the illumination, the use of tungsten illumination produces an apparent increase in the damage rate relative to sunlight. However, because the solar spectrum and the tungsten spectrum are well known, measurement of the spectral response and the I-V characteristics under a known spectrum are the required measurements. The complications and uncertainties associated with the use of solar simulators for solar cell experiments conclusively establishes a simple, well-known light source for these experiments. The principal liability attendant to the use of a 2800°K tungsten spectrum for radiation damage studies is the capricious misinterpretation of the tungsten data.

In an effort to simulate experimentally, for illustrative purposes, the difference between the standard tungsten light spectrum and the sun spectrum, the electrical characteristics of the solar cells were measured under two different illumination conditions in this experiment. The primary source of light used was a bank of 2800°K tungsten floodlamps without any filtering, while a second set of measurements was obtained using a bank of 3400°K tungsten photofloodlamps with a two-inch water filter between the lamps and the illumination plane. This latter

not exceed the limits of the H and D curve. The proportional proton intensity, as determined by the film, was integrated over the active area of the secondary emission monitor. (The active area could be visually determined by placing a film on the back of the secondary emission monitor and using the proton beam to obtain a radiograph.) Over 98 per cent of the beam was contained within the active area, consequently, proton scattering from the sides of the secondary emission monitor did not contribute significantly to the output of the monitor. The proton flux on the specimens was determined by distributing the total beam as measured by the secondary emission monitor according to the results of the densitometric analysis.

We are mindful of the errors attendant to the flux determination outlined above. In all but these experiments, reliance has been placed upon C^{11} activation. However, the 740 Mev data included herein were obtained by the film method. Considerable attention was given to C^{11} and film comparisons in later experiments in order to establish the uncertainty limits and discover any systematic errors. The proton intensities can be shown to be accurate to better than 50 per cent. Our best estimate of the uncertainty is 20 per cent, but these lower limits cannot be established conclusively.

The solar cells used in this experiment consisted of Hoffman p on n 9 per cent ungridded and 11 per cent gridded 1 x 2 cm silicon solar cells. These cells were commercially available items in which the efficiencies quoted were obtained under tungsten light and, therefore, nominally classed as 9-10 per cent and 11-12 per cent cells. In addition, three of the Evans Signal Laboratories' experimental n on p silicon solar cells having efficiencies of 6-7 per cent were supplied by W. Cherry of U.S. Army Signal Research and Development Laboratory.

On each of the experimental solar cells, I-V characteristics and short circuit current were measured prior to, immediately after, and for various subsequent periods of time after the irradiation. The technique used to measure these electrical characteristics consisted of illumination with tungsten light and graphically recording the electrical

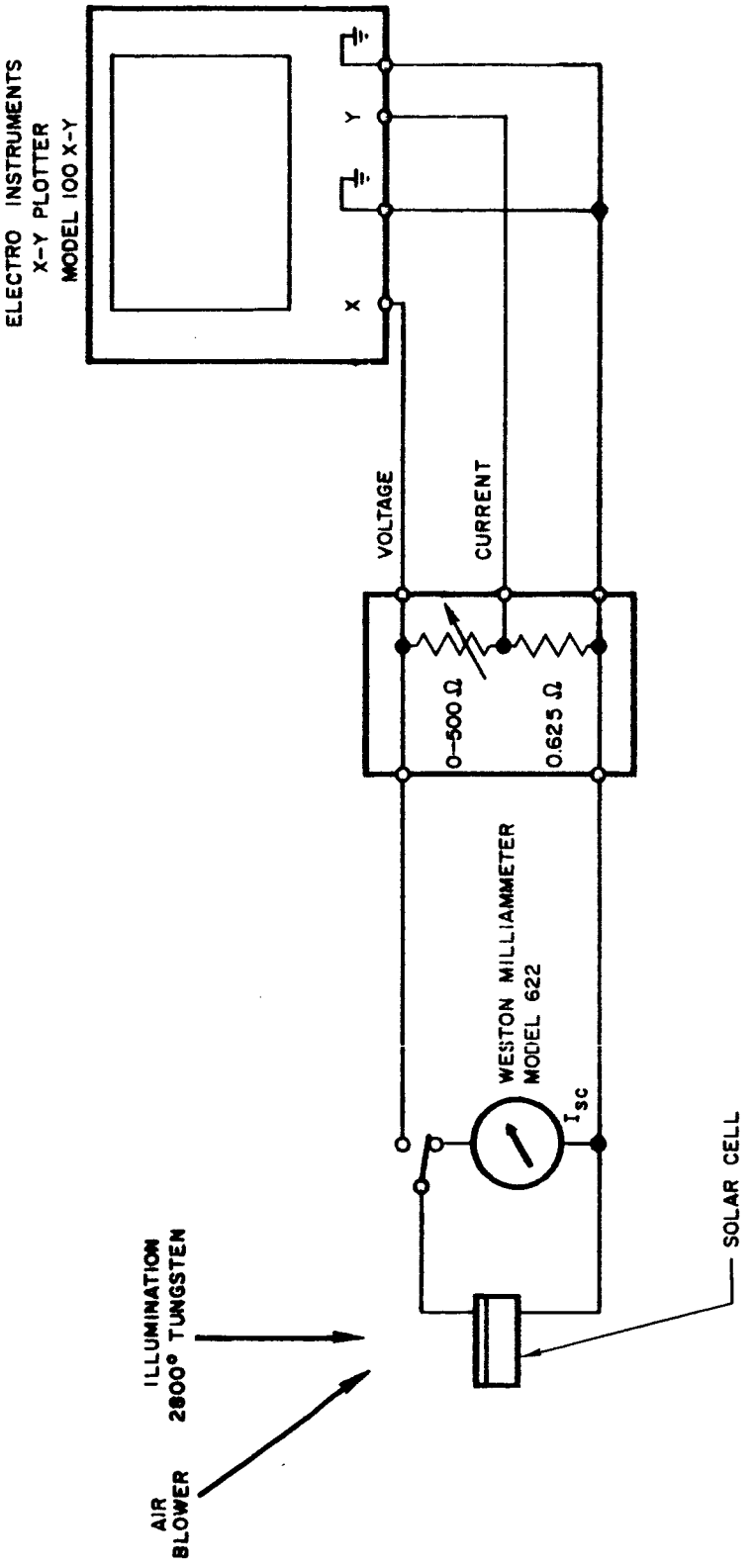

Figure 1. Short Circuit Current and I-V Characteristic Measurement

light source more closely approximates the sun spectrum in that the higher operating temperature of the lamp filaments increases the short wavelength output while the two-inch water filter greatly attenuates the long wavelength component. This latter light source, however, is not an accurate sun simulator and, being extremely cumbersome and complex, does not provide the portability and reproducibility necessary for the experimental techniques utilized here. On this basis, the 2800°K unfiltered tungsten spectrum was used in this and following experiments as a standard light source for radiation damage measurements. Extrapolation of these data to operation in the sun spectrum is discussed in detail in another report.

In order to determine the nature of the radiation produced damage in the solar cells and to acquire additional information for the extrapolation of the data to predictions of performance under sun illumination, spectral response characteristics of the solar cells were measured before and after irradiation. The measurements were made with a Perkin-Elmer double-pass prism monochromator suitably modified to provide higher accuracy in the short wavelength regions. The calibration of the output energy supplied by the monochromator was determined by a standard thermocouple detector. The use of several of these thermocouple detectors as calibrated sources allowed reproducibility of the relative output energy to within $\pm$ 10 per cent. In this manner, it was possible to determine accurately the relative absolute reduction in spectral response in all of the test specimens. Having acquired the change in spectral response of the solar cells, this change can be integrated with either the tungsten light spectrum or the sun spectrum to obtain the per cent reduction in short circuit current for a given amount of radiation damage under either light spectrum.

The experimental solar cells were mounted on flat aluminum plates placed perpendicular to the proton beam. The beam distribution was sufficiently large that five test specimens could be placed in the beam at one time with a variation in proton flux across the area occupied by the test cells of only $\pm$ 5 per cent. The secondary emission monitor was placed behind the plate of experimental test cells, Figure 2. At 740 Mev, a negligible percentage of the incident proton beam is stopped or

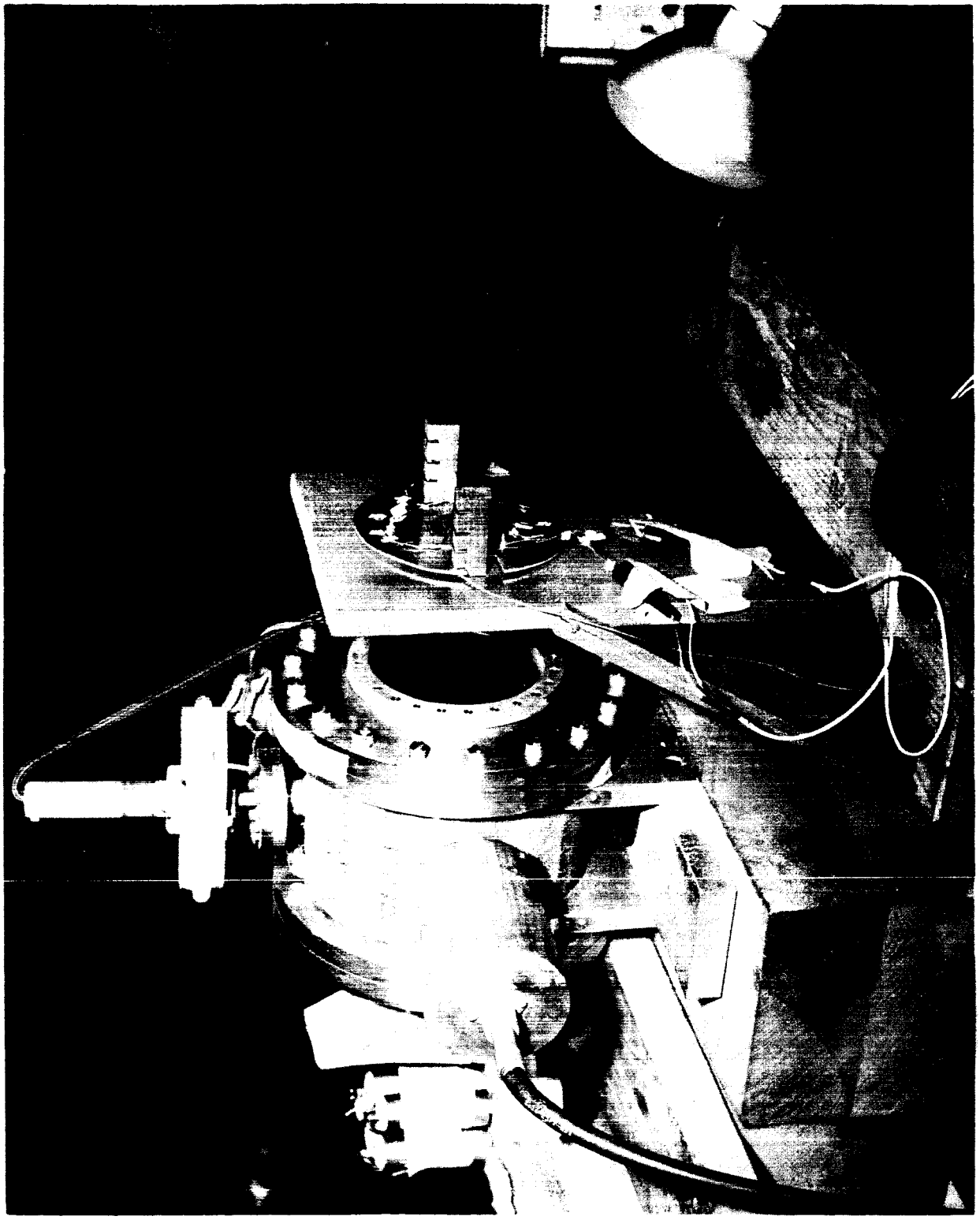

Figure 2. Solar Cell Irradiation
Experimental Arrangement

scattered at a sufficiently large angle to avoid entering the secondary emission monitor. In each irradiation, the cells were illuminated with 2800°K tungsten light and the short circuit current of two specimens was remotely monitored during the irradiation on strip chart recorders, Figure 3. The solar cells were cooled during illumination with an air blower. Temperature measurements under conditions of irradiation and illumination indicated that the solar cells remained at 75 $\pm$ 2°F throughout the test. These measurements allowed determination of dynamic response of the cells as a function of integrated flux and also served to determine if any solar cell recovery or annealing were evident after cessation of the proton beam. Due to low line voltage in the proton beam cave, the illuminating lamps were not operated at full rated power resulting in a slightly larger long wavelength component which accentuated the measurements of short circuit current degradation during irradiation. These data are suitably designated in order to distinguish them from true 2800°K illumination.

In addition to the exposure of the cells to the primary beam, a series of experiments were conducted in which some of the cells were shielded with 4.32 grams/cm^2 of lead, quartz, and aluminum to determine if any secondary processes, such as low energy nucleon scattering from the shields, were present. In each case, the shields were placed directly in front of the solar cells. The corresponding shield thicknesses were 0.38 cm of lead, 1.87 cm of quartz, and 1.60 cm of aluminum.

2.2 450 and 400 Mev Experiments

The 450 and 400 Mev experiments were conducted in the synchrocyclotron at the University of Chicago. The cyclotron was operated under external beam conditions providing a proton beam current of about 1 x 10^{-9} amperes over an area of approximately 1½ square inches. The total beam current was measured by a secondary emission monitor of the Tautfest type[1] which was designed and built at the University of Chicago. The monitor, having a large sensitive area, was placed outside the beam port in back of the experimental setup in a manner similar to the previously described experiment at the University of California. The monitor was calibrated by establishing a ratio between its reading and the reading of an argon filled ionization chamber simultaneously. The ionization chamber was calibrated with scintillation counters by establishing counting ratios between counters in the beam and counters looking at the beam after

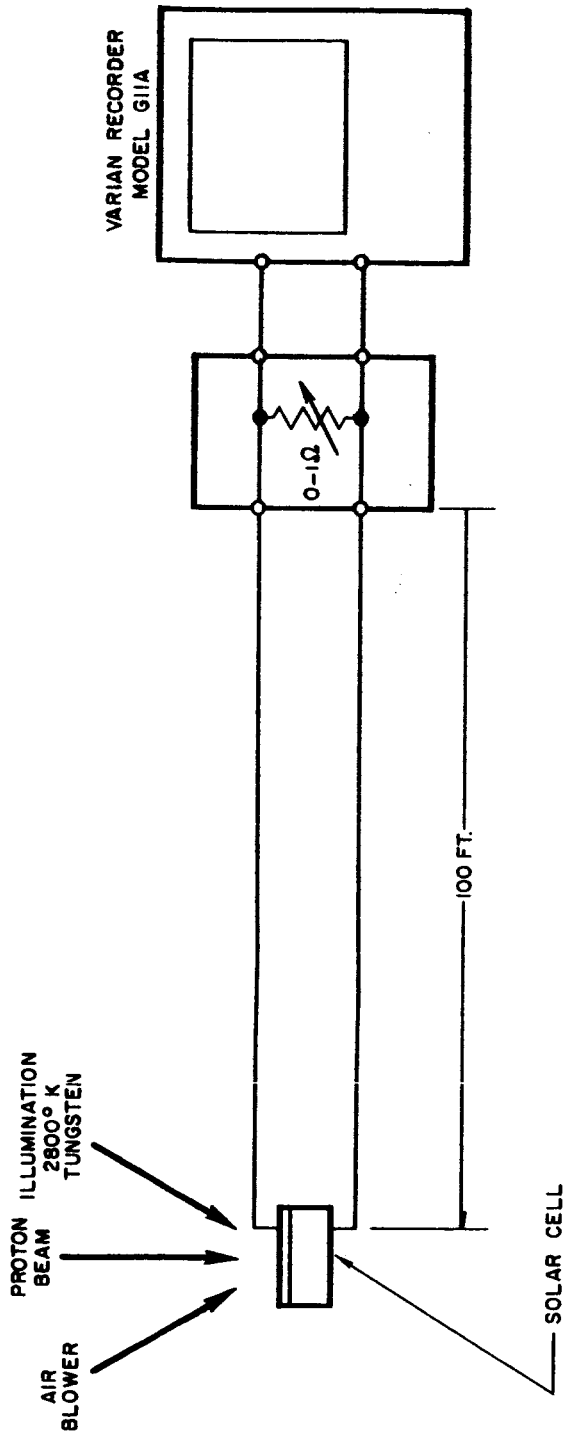

Figure 3. Short Circuit Current Measurement During Irradiation

multiple scattering in two inches of lead. The output of the secondary emission monitor was integrated during the experiment to provide the total integrated beam current. Similar to the previous experiment at 740 Mev, x-ray films were utilized to set up the proper beam alignment and beam focus conditions. A $\frac{1}{2}$-inch thick slab of polyethylene was inserted in the external beam tube to aid in defocusing the beam through small angle scattering. The polyethylene slab was located 18 feet from the exit end of the external beam tube to insure that no low energy protons reached the solar cells under irradiation.

After beam alignment and focus had been achieved, two techniques were utilized to obtain the beam distribution. The first consisted of exposing a series of x-ray films as in the 740 Mev experiment. The optical transmission of these films was measured; using standard H and D curves, the relative exposure across the beam area was determined in a manner identical to that used in the 740 Mev experiment. In addition to the x-ray film densitometric analysis, C^{11} activations were performed. This technique consists of exposing a carefully positioned 1/16-inch thick sheet of polyethylene in the beam for a period of five minutes. The sheet of polyethylene was cut into 1 cm x 1 cm sections and the activation of these sections was determined with a GM tube and scaler. After correcting the observed count rates for the 20.5 minute half-life of C^{11}, the initial activation, which is proportional to the total exposure, can be determined. Using the relative values of the activations of the incremental areas in conjunction with the measurements obtained with the secondary emission monitor, the beam flux was determined for each incremental area. Comparison of the beam profiles obtained with the C^{11} activation technique and densitometric analysis of the x-ray films indicated that, as had been observed in the previous experiment at 740 Mev, the information obtained through the use of x-ray films was inferior in view of the large range of exposures across the beam area. C^{11} activation was taken to be indicative of the beam profile, and deviations of the results of the x-ray film analysis from the C^{11} activation analysis were used to cross check the integrated fluxes previously obtained in the 740 Mev experiment at Berkeley. Because the accuracy of the beam distribution determination with the C^{11} technique exceeds the accuracy of the total beam measurement, the over-all flux determination is estimated to be accurate to within $\pm$ 5 per cent.

The solar cells irradiated in this experiment consisted of Hoffman p on n 9 per cent ungridded and 11 per cent gridded 1 x 2 cm silicon solar cells of the same type used in the experiment at 740 Mev. In addition, a series of matched 1 cm x 1 cm p on n Hoffman solar cells were used. These half-cells were prepared by taking a 1 x 2 cm cell, cutting it in half and gridding one of the two halves. This group of cells was prepared to determine if the degradation of short circuit current was dependent upon the gridding of the solar cells. A series of n on p silicon solar cells, consisting of specimens from Transitron, Texas Instruments, Hoffman, and BTL, were also irradiated. In addition, four gallium arsenide experimental solar cells furnished by RCA were included in the experiments.

On each of the test solar cells, I-V characteristics, short circuit current, and spectral response were measured before and after the irradiation. In addition, two solar cells were monitored during the irradiation with strip chart recorders. The measurement techniques used to determine these electrical characteristics were the same as those used in the 740 Mev experiment. The illumination source was in all cases a 2800^{o}K unfiltered tungsten light spectrum. In this experiment, two 1 kw Sola line regulators were used to maintain the illumination sources for pre and postirradiation measurements and short circuit current measurements during irradiation at operating power levels, thus eliminating differences in measurements due to unequal tungsten light spectra.

The solar cells were mounted on flat aluminum plates in a manner similar to that used in the 740 Mev experiment. The beam area, however, was only sufficiently large enough to allow the irradiation of two solar cells per run. The physical arrangement of the solar cells, the specimen plate holder, and the secondary emission monitor was the same as in the previously described 740 Mev experiment.

The external intermediate focus occurs in air in the Chicago cyclotron. Insertion of about 18 inches of lithium hydride (kindly provided by Professor L. Pondrum of Columbia University) and refocusing, an external beam of 400 Mev, $\pm$ 0.5 Mev, was obtained. Proton

energy was determined by magnetic analysis and confirmed by range-energy calculations. Efforts to achieve lower energy beams by inserting more effective copper absorbers at the intermediate focus were not fruitful. Only 450 Mev and 400 Mev data were successfully obtained.

2.3 20.5 Mev Experiments

The 20.5 Mev proton experiments were conducted in the 20 Mev synchrocyclotron at UCLA. The cyclotron was operated with an external proton beam current of about 10^{-9} amperes over a region approximately $\frac{1}{2}$-inch wide x 4-inches long. Alignment of the test specimen was accomplished through film exposure as previously described. Due to machine instability, in that an external beam current could not be reproduced in successive runs, it was necessary to acquire proton flux simultaneously with the solar cell irradiations. Since the range of 20 Mev protons is only of the order of 550 mg/cm^2, a Faraday cup was used. The experiments were performed in an evacuated chamber, Figure 4, which contained a 1 x 2 cm chip of steel 0.1-inch thick as a collector. The solar cell to be irradiated was mounted on a chip and the protons striking the cell penetrate the cell and are stopped in the steel chip. A current integrator was used to measure the beam current collected by the chip which, having the same area as the test cell, resulted in a value of integrated proton flux incident on the solar cell under irradiation. The test cells and collector chips, which were glued together, were held in a fixed position on a phenolic insulator in the chamber by a small magnet buried in the phenolic insulator. The chamber was maintained at fore pump vacuum of approximately 20 microns during the irradiation period. A series of tests in which the indicated collector current was measured as a function of chamber pressure indicated that a pressure of 20 microns was sufficient to remove measurable ionization effects in the measured beam current.

The vacuum chamber consisted of three electrical feed-throughs for beam current, grid voltage, and solar cell current signals. Since the cells were not illuminated with light, the measurement of solar cell current under irradiation allowed a quantitative check on the collector beam current readings. In this configuration, the solar cell

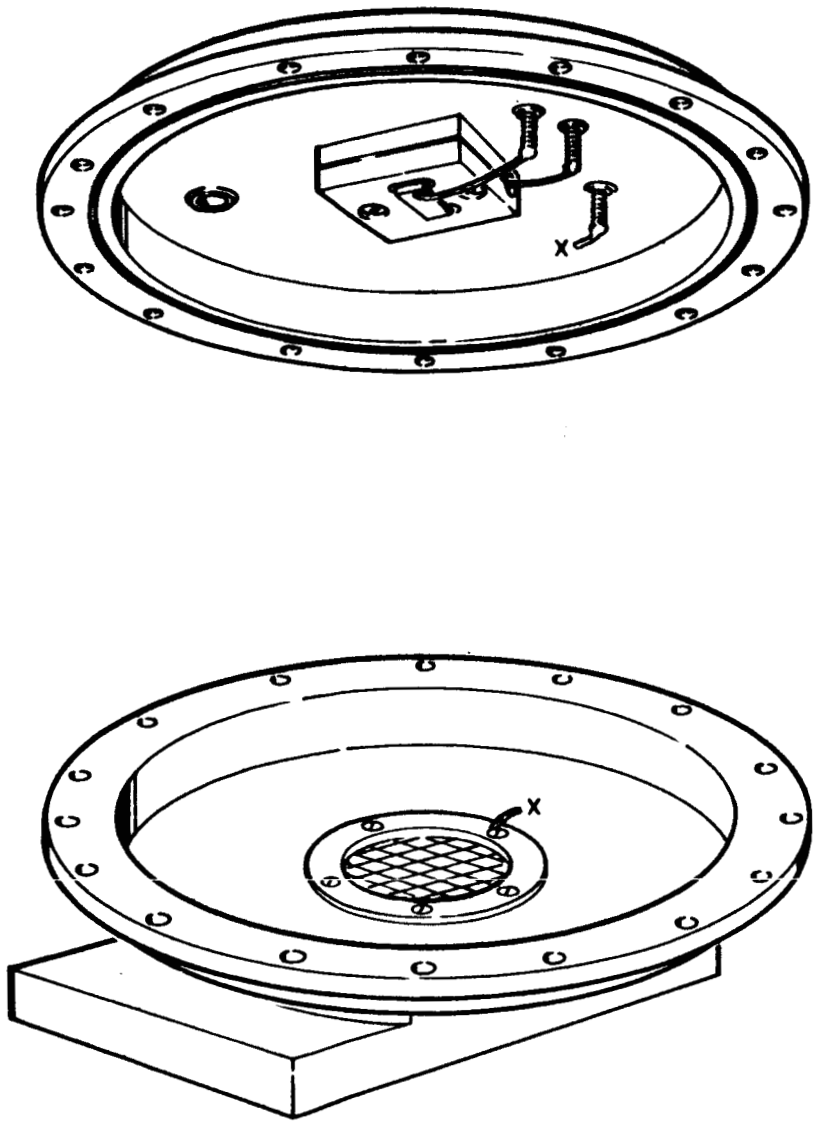

Figure 4. Irradiation Chamber for
20.5 Mev Proton Experiments

acts as a solid-state detector. The output current of the cell is dependent upon the number of incident protons per unit area, the number of hole-electron pairs generated per unit path length, and the minority carrier diffusion length. Using an already heavily damaged cell of known minority carrier diffusion length to eliminate damage during the measurements, and knowing the carrier generation rate from the incident proton energy, measurement of cell current readily yields the incident proton flux. The direct measurements of proton flux agreed within 25 per cent with the proton fluxes obtained through collector current measurements.

After the first series of irradiations, a grid was interposed between the chamber window and the test specimen and collector to determine if the measured beam current was affected by forward scattered particles in the 5 mil aluminum window or by back scatter off the solar cell and collector. These measurements indicated that the measured beam currents were of the order of 25 per cent higher than the actual beam currents. There were, however, additional indications that some leakage existed between the collector chip and ground through the phenolic insulator due to ionization produced in the phenolic insulator by the incident beam. This latter effect would result in a measured beam current which was less than the actual beam current. Since these two effects tend to cancel, the net accuracy of the measured integrated proton flux is estimated to be better than $\pm$ 25 per cent.

The solar cells irradiated in this experiment consisted of Hoffman p on n 9 per cent ungridded silicon solar cells from the same lot as used in the experiments at Chicago; Hoffman p on n shallow diffused solar cells made from both oxygen-free transistor grade silicon and standard solar grade silicon; Heliotek p on n shallow diffused solar cells made from both oxygen-free and standard solar grade silicon; BTL n on p shallow diffused solar cells made from standard solar grade silicon; and Hoffman n on p shallow diffused solar cells made from oxygen-free transistor grade silicon. Thus, this spectrum of test specimens allowed the acquisition of data for the following:

1. Comparison of solar cells made from oxygen-free material with cells made from standard solar grade material for both p on n and n on p cells.

2. Comparison of solar cells having shallow diffused junctions of the order of $\frac{1}{2}$ micron diffusion depth with standard commercially available solar cells having diffusion depths of the order of one to two microns.

3. Comparison of solar cells having the same material and electrical characteristics but produced by different companies.

The electrical measurements made on these solar cells were identical with the measurements previously described for the 740 and 450 Mev experiments. The only exception to the group of previously mentioned electrical measurements is that, due to the irradiation in the vacuum chamber, no measurements were made of degradation of short circuit current during irradiation.

Due to the wider spectrum of solar cell types used in this experiment, a larger variance of spectral response characteristics was obtained. Since the short circuit measurements were made under tungsten light, it should be kept in mind that, when comparing different types of cells as to their radiation sensitivity under sun illumination, the analysis of spectral response curves plays an important role.

The experimental setup was partly described in the previous discussion of dosimetry inasmuch as the solar cell mounting arrangement was an integral part of the beam current measurements. Due to the narrow width of the beam and the large uncertainties in beam flux at the external ends of the beam profile, it was possible to irradiate only one cell at a time. The chamber, Figure 4, was clamped to the end of the external beam port and the protons entered the chamber through a 0.005-inch aluminum vacuum window. Changing of the test specimens was accomplished by breaking the vacuum, removing the front end of the chamber for specimen mounting, and reassembly followed by evacuation to fore pump pressure.

3.0 EXPERIMENTAL RESULTS

The radiation damage data obtained in a variety of experiments described in this report served two principal objectives: investigation of the energy dependence of proton damage and investigation of the factors related to solar cell damage. This report considers the latter point; the energy dependence is described in a separate report.

3.1 740 Mev Experiments

The degradation of silicon solar cell short circuit current illuminated with 2800°K tungsten light as a function of integrated proton flux is shown in Figure 5. Each point indicated in this and following figures represents an individual solar cell. The initial short circuit currents for all the solar cells were about 25 ma/cm^2 for 100 mw/cm^2 illumination. It is evident that the rate of degradation of short circuit current is linear with the log of the integrated flux. This logrithmic dependence is due to the exponential absorption characteristics of light in silicon. There is a slight difference in radiation sensitivity between the Hoffman p on n 11 per cent gridded and the 9 per cent ungridded cells in that the former appeared to be slightly more sensitive to radiation. This apparent difference is inconsistent with the theory of operation of silicon solar cells in that the only effect of the gridding is the increase in available power output through reduction of the p-layer resistivity which has no effect on short circuit current. The value of integrated proton flux required to reduce the initial short circuit current by 25 per cent is shown to be 8×10^{10} p/cm^2. Illumination of the same cells with a 3400°K water filtered tungsten light spectrum indicates a reduced sensitivity in that 25 per cent degradation occurs at an integrated flux of about 2×10^{11} p/cm^2, Figure 6. This difference indicates that the radiation damage is not uniform over the spectral response of the solar cells. Measurements of the short circuit current during irradiation agree with the data obtained in pre and postirradiation measurements after correcting for the low line voltage in the beam cave.

Later measurements of postirradiation short circuit currents indicate that negligible short-time annealing effects occurred. Further,

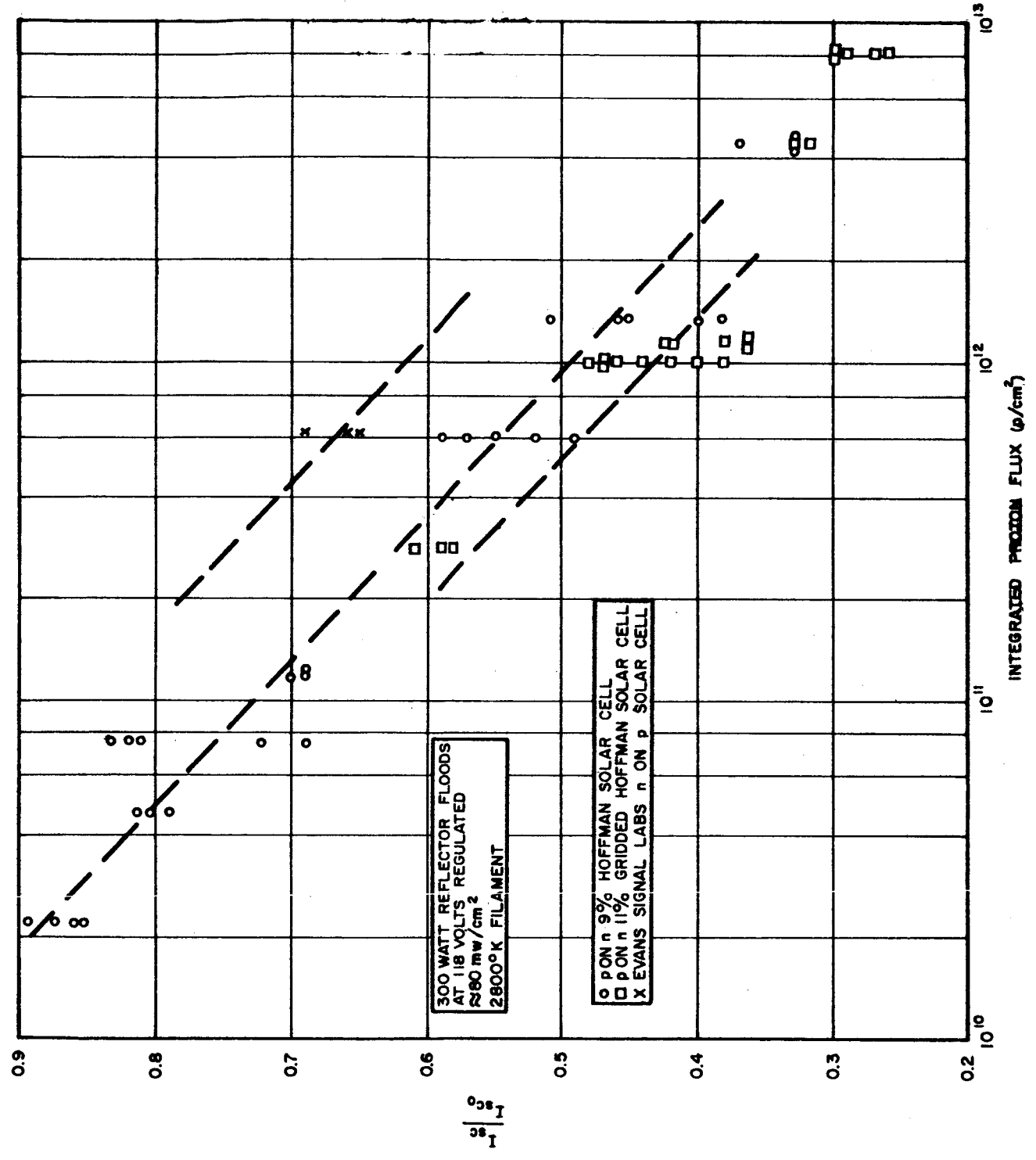

Figure 5. P on N Silicon Solar Cell Short Circuit Current Degradation With 740 Mev Protons - 2800°K Illumination

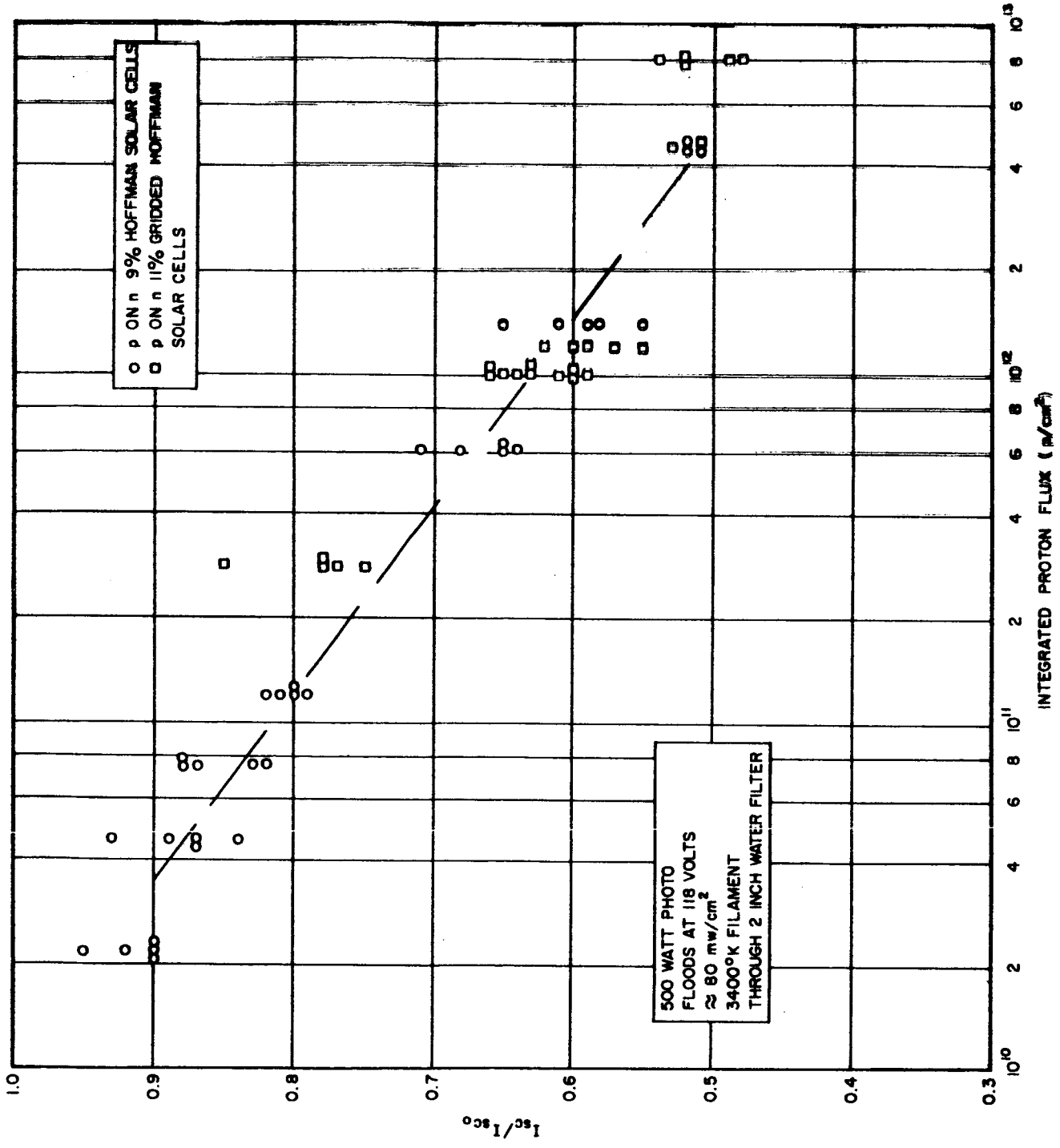

Figure 6. P on N Silicon Solar Cell Short Circuit Current Degradation With 740 Mev Protons - 3400°K Illumination

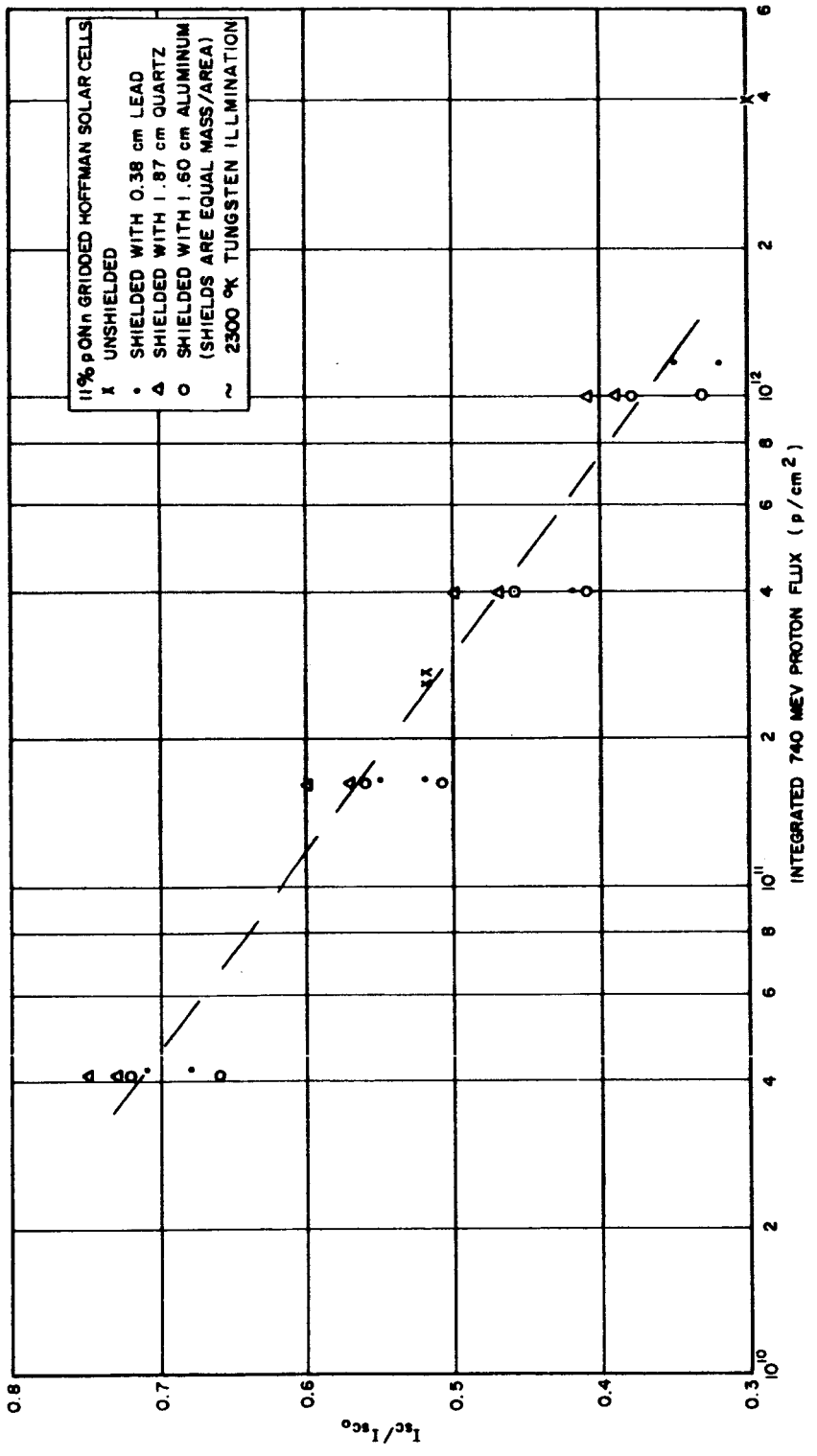

Figure 7. Effect of Shielding on Short Circuit Current Degradation With 740 Mev Protons

for these particular solar cells, no annealing at room temperature existed. Additional isochronal annealing experiments showed that negligible amounts of damage recovery occurred below temperatures of about 200°C which is in agreement with previous work conducted by Bemski and Augustniak[2].

In the irradiations using lead, aluminum, and quartz shielding in front of the solar cells under irradiation, the degradation of short circuit current as a function of integrated proton flux followed the same general pattern as observed without the shields, Figure 7. Since negligible energy loss is involved in the passage of 740 Mev protons through shields of the thicknesses used, these data seem to indicate that no significant secondary processes are occurring under these conditions. The data shown in Figure 7 were acquired under illumination with the light source in the beam cave. Since this illumination source was not operated at full rated power, due to low line voltage in the beam cave, the long wavelength component was relatively higher resulting in accentuated damage rates. Thus, these data, which are uncorrected for the low filament temperature, indicate 25 per cent damage at 3×10^{10} p/cm^2 compared with 8×10^{10} p/cm^2 under 2800°K tungsten illumination.

The effect of the proton irradiation on the I-V characteristics of silicon solar cells is shown in Figure 8 for the ungridded 9 per cent cells and Figure 9 for the gridded 11 per cent solar cells. These data were obtained under 3400°K tungsten water filtered illumination and, therefore, are consistent with the short circuit current degradation under the same light spectra as shown previously in Figure 6. Since all the I-V characteristics indicate similar degradation shapes, the curves shown here illustrate only a few typical values of response. Several points of interest are evident: (1) the short circuit current degrades considerably more rapidly than open circuit voltage, (2) the degradation of maximum power output is approximately equal to the degradation in short circuit current, and (3) the degradation in output power as a function of integrated flux will depend strongly upon the load line utilized in a particular application. Since the I-V characteristic shape is independent of the light spectrum used in the illumination of the solar cells, the I-V characteristics obtained under 2800°K tungsten illu-

---

[2] G. Bemski and W. M. Augustniak, Physical Review, Vol. 108, No. 3, 645, (1957)

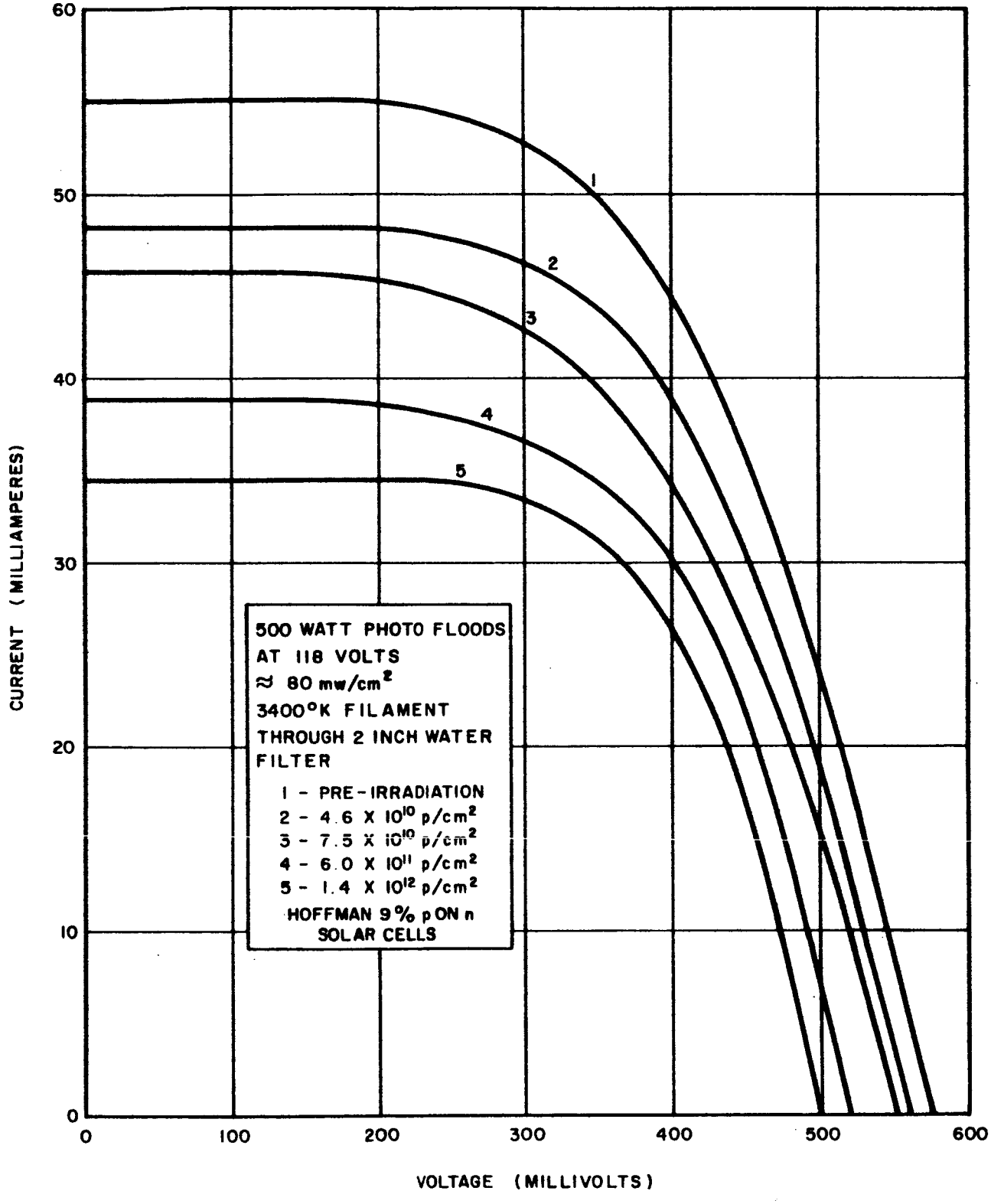

Figure 8. P on N Silicon Solar Cell I-V Characteristic Degradation With 740 Mev Protons

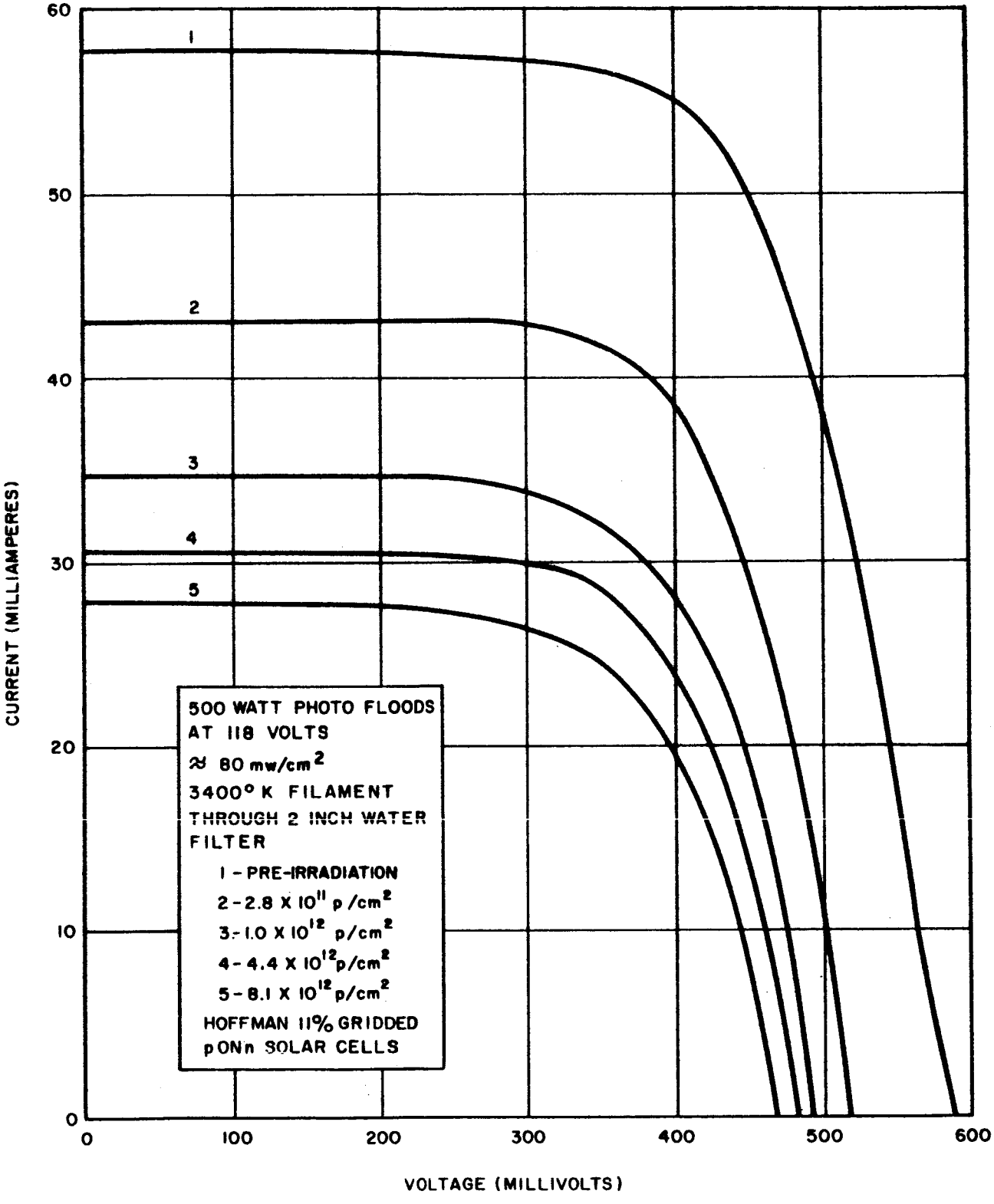

Figure 9. P on N Gridded Silicon Solar Cell I-V Characteristic Degradation With 740 Mev Protons

mination are identical with those shown in Figures 8 and 9 with the exception of the dependence of the short circuit current versus integrated flux on the incident light spectra. Hence, it is only necessary to determine the short circuit current for given values of integrated flux and a given incident light spectrum in order to acquire a family of I-V characteristics for analysis of degradation in output power under particular load conditions.

The irradiation of the three n on p Evans Signal Laboratory silicon solar cells indicated that at 740 Mev the sensitivity of these n on p cells was about a factor of three less than the p on n cells under 2800°K tungsten illumination. These data for the n on p solar cells are plotted in Figure 5 along with the p on n solar cell data. The I-V characteristics of these particular cells as a function of integrated flux are identical with the p on n cells in that the shape of the I-V characteristic is primarily dependent on degradation in short circuit currents. Since only a few of these cells were obtainable at the time of the irradiation, it was not possible to obtain good statistical data as in the case of the p on n cells; however, the three cells that were irradiated yielded consistent data.

The spectral response characteristics of the solar cells irradiated in this experiment were measured before and after irradiation to determine the nature of the short circuit current degradation and to allow the extrapolation of short circuit current degradation for any given integrated flux to a particular light spectrum of interest. The effect of the proton irradiation on the spectral response characteristics of the solar cells was similar in all cases, as indicated in Figures 10 and 11 for p on n silicon solar cells. Since the effect of gridding is only evidenced in the region of maximum power output, the spectral response characteristics of the gridded and ungridded cells are identical due to the fact that the response curves are obtained under short circuit current conditions. As was the case of the shape of the I-V characteristic, the shape of the spectral response as a function of integrated flux plays an important role in the determination of output power degradation. As is evident in Figure 10, the primary effect of proton irradiation is a decrease in the long wavelength response of the

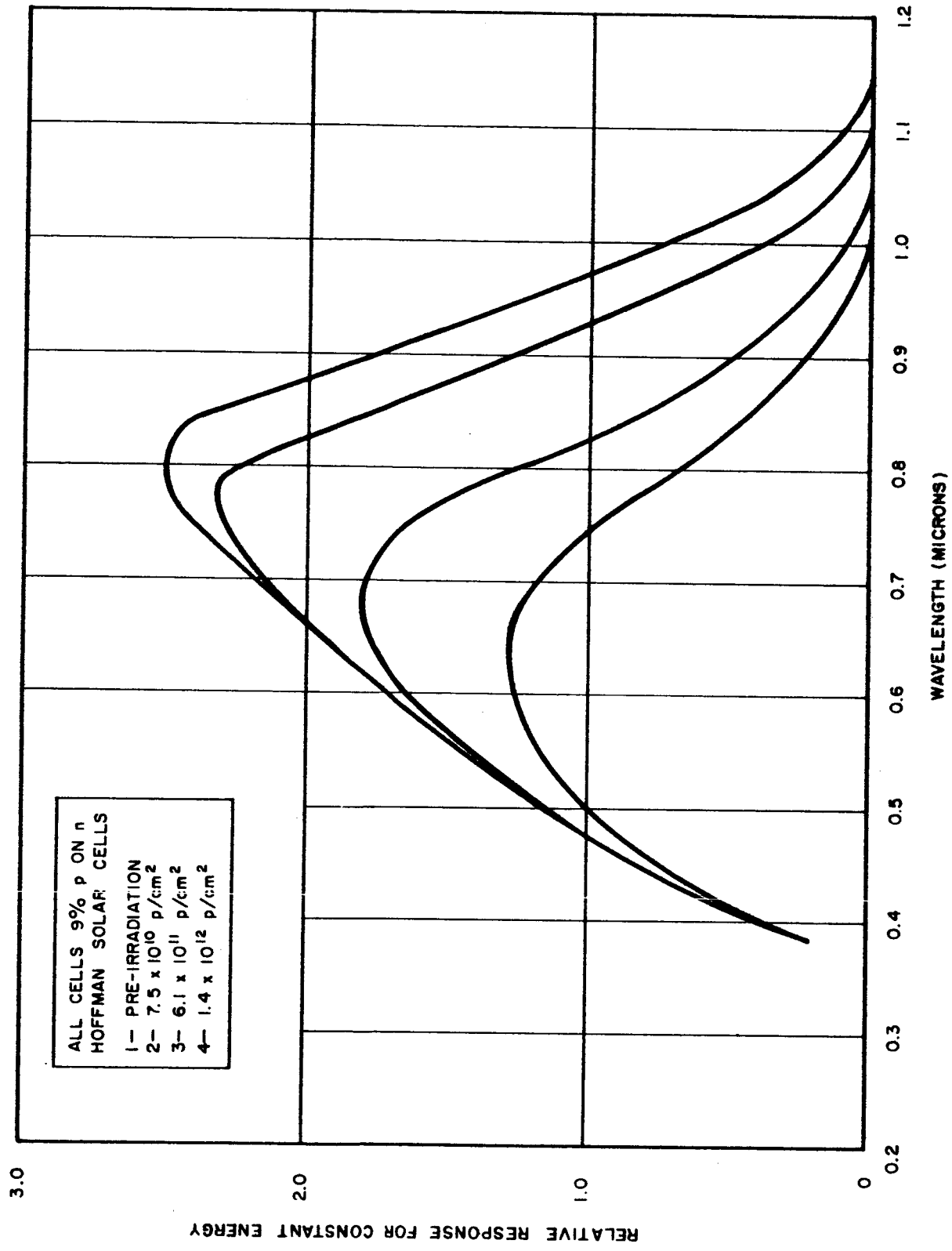

Figure 10. P on N Silicon Solar Cell Spectral Response Degradation With 740 Mev Protons

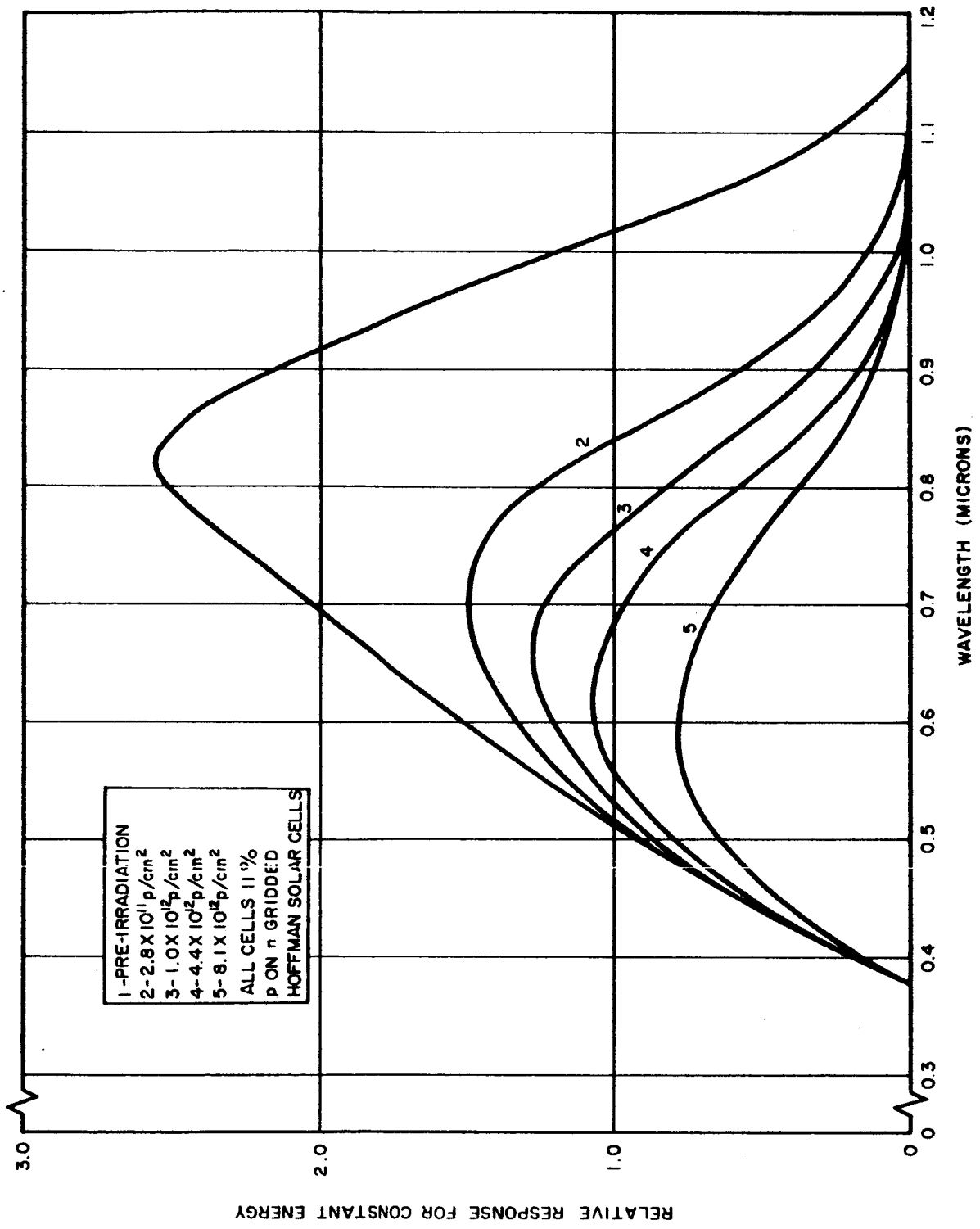

Figure 11. P on N Gridded Silicon Solar Cell Spectral Response Degradation With 740 Mev Protons

solar cell which explains the apparent increased damage rate under 2800°K tungsten light compared to the 3400°K water filtered tungsten light. The decrease in long wavelength response is due to the reduction of minority carrier lifetime in the parent material of the solar cell which limits the depth below the junction from which photon generated carriers can be collected. There appears to be little change in the spectral response curves in the short wavelength region which indicates that the proton radiation has little effect on the carriers generated near the surface of the solar cell. Since the spectrum of sunlight is strongly peaked in the 500 millimicron region, the degradation of solar cell electrical characteristics under sun illumination will not be as severe as is indicated by the data acquired under illumination by tungsten light. The extrapolation of the data presented here to the degradation of solar cells in space under sun illumination is discussed in another report and will, therefore, not be considered in further detail.

3.2 450 Mev Experiments

As in the case of the 740 Mev proton irradiations, the rate at which 450 Mev protons degrade the electrical characteristics of silicon solar cells is considerably higher than would be predicted on the basis of simple displacement theory through Rutherford scattering. The data, however, are generally in quantitative agreement with the data obtained in the 740 Mev experiment. Additional data were obtained on n on p solar cells and on the effect of the gridding on solar cell sensitivity to proton radiation.

The electrical characteristics of the solar cells irradiated in this experiment were obtained using only a standard 2800°K unfiltered tungsten light spectrum of about 110 mw/cm^2, since data obtained on spectral response characteristics allow extrapolation to any light spectrum of interest. The rate of short circuit current degradation as a function of the log of the integrated flux, Figures 12 and 13, is linear and exhibits approximately the same slope as was evidenced in the previous experiment at 740 Mev. In Figure 12, the degradation of short circuit current is shown for 9 per cent ungridded p on n cells and 11 per cent gridded p on n cells obtained from Hoffman as commercially available specimens. The cells, however, were produced at a different time and,

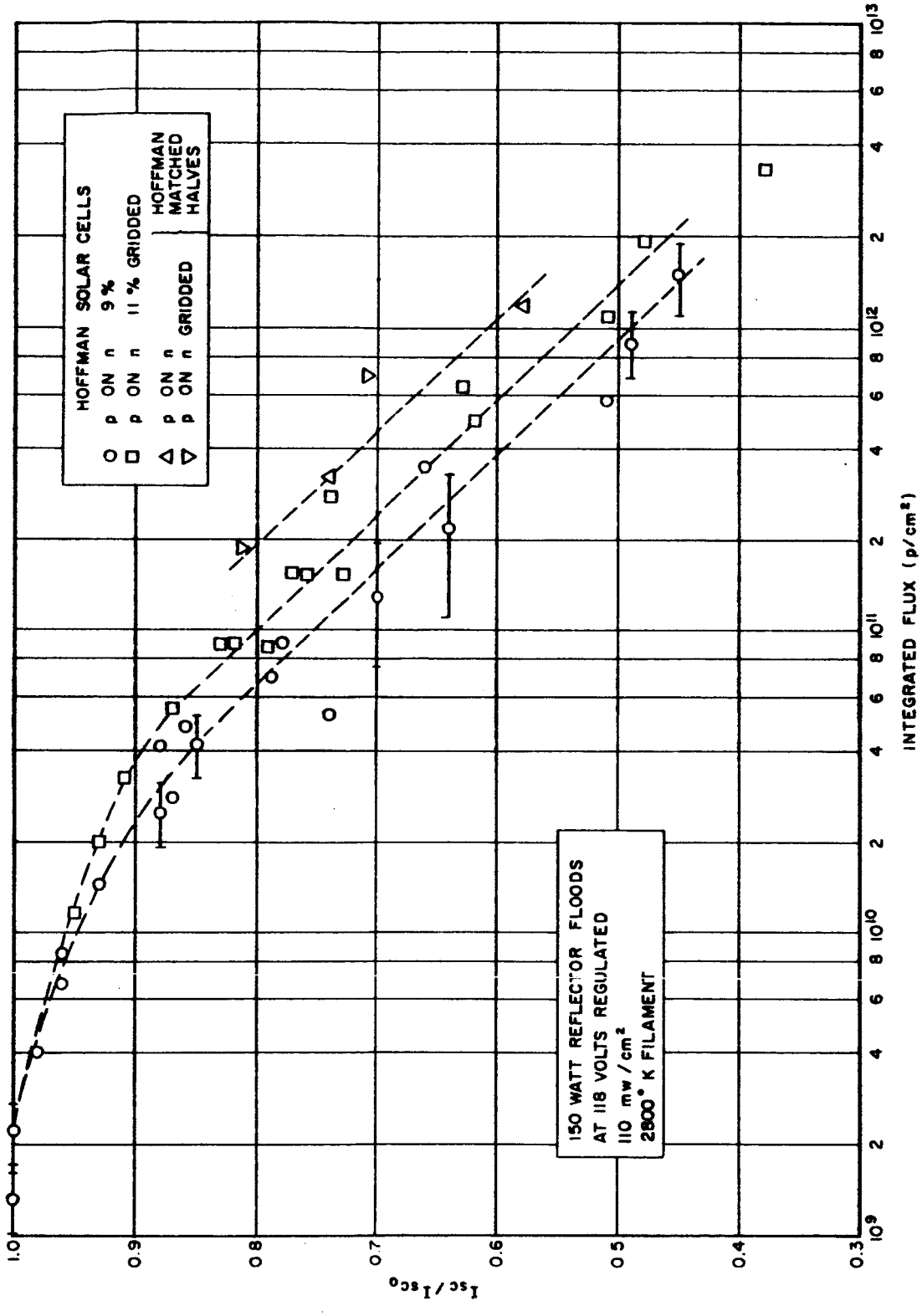

Figure 12. P on N Silicon Solar Cell Short Circuit Current Degradation With 450 Mev Protons

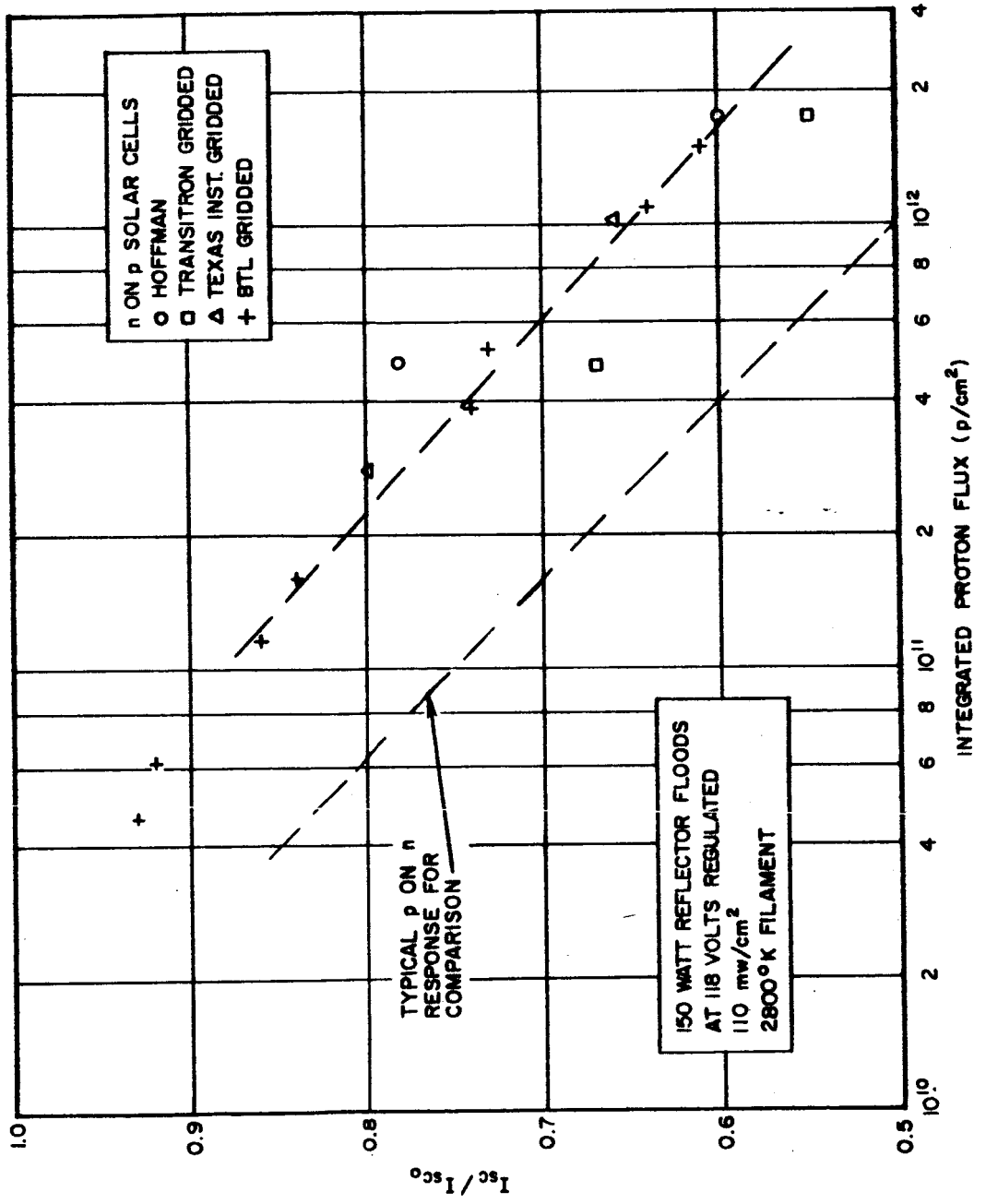

Figure 13. N on P Silicon Solar Cell Short Circuit Current Degradation With 450 Mev Protons

therefore, were not acquired from the same lot as the cells previously irradiated at 740 Mev. It is of interest to note that, in contradiction with the data previously obtained, the ungridded cells appear slightly more sensitive than the gridded cells. Inasmuch as these cells were electrically identical with the cells previously irradiated at 740 Mev, it is evident that some unidentified material characteristic controls the rate of degradation of solar cells under high energy proton bombardment. In addition, the response of several matched pairs of gridded and ungridded p on n cells to proton irradiation is shown in Figure 12 which indicates that gridding has no effect on the degradation of short circuit current under proton bombardment. It is important to recognize that the data shown in these figures (Figures 5, 12 and 13) are representative of commercial p on n cells, but that individual cells may require a variation in integrated flux of a factor of two in order to exhibit the same degradation. This variation depends upon a number of factors, including purity of parent material and depth of boron diffusion.

The p on n ungridded cells indicate 25 per cent damage at an integrated flux of 1×10^{11} p/cm^2, in agreement with the previous experiment at 740 Mev, while the gridded cells indicate 25 per cent damage at 1.5×10^{11} p/cm^2. The n on p silicon solar cells, including specimens obtained from Hoffman, Texas Instruments, Transitron, and BTL, indicate 25 per cent degradation in short circuit current at about 4×10^{11} p/cm^2, Figure 13. These data exhibit the same slope under tungsten light as do the p on n cells and appear less sensitive to radiation by a factor of three to four which is consistent with the data acquired at 740 Mev. There appears to be little difference in sensitivity between manufacturers, indicating that production techniques alone do not play an important role in the sensitivity of these cells to radiation. In addition, four gallium arsenide solar cells supplied by RCA were irradiated to 1.7×10^{12} p/cm^2 without exhibiting any measurable change in electrical characteristics. These cells, however, had initial efficiencies only of the order of 2 to 3 per cent under sun illumination. It cannot be concluded from these data that gallium arsenide cells possess any advantage over silicon cells. Silicon cells with similar initial efficiencies (2 to 3 per cent) and similar minority carrier lifetimes also would not exhibit any radiation damage. Refer, for example, to Figure 12; if a

silicon cell had been exposed to $\sim$ 1-3 x 10^{13} p/cm^2 yielding an efficiency of $\sim$ 3 per cent before beginning the experiment, an additional exposure of 1.7 x 10^{12} p/cm^2 would have produced no further change.

The I-V characteristics obtained for both the p on n and n on p solar cells exhibit the same general degradation in shape as did the I-V characteristics obtained in the 740 Mev experiment. Figures 14 and 15 illustrate typical sets of I-V characteristics for gridded n on p cells as a function of integrated flux. Similar to the 740 Mev experiment, the short circuit current is more rapidly affected by radiation than the open circuit voltage and the degradation in the maximum power output closely follows the degradation in short circuit current.

Since the results of the annealing experiments performed on the solar cells irradiated at 740 Mev were negative, there were no detailed annealing experiments performed on the solar cells irradiated at 450 Mev. However, in the process of conducting calibration experiments several months later, qualitative evidence of annealing was observed on some of the n on p solar cells. Extensive measurements on all the solar cells irradiated in the 450 Mev experiment indicated that some of the n on p solar cells had recovered 15 to 25 per cent of their short circuit current reduction. During this interim period of time, the cells had been stored at room temperature. Most of the p on n cells irradiated at Chicago were reinvestigated and a small amount of recovery ($\sim$5 per cent) was found in some of them. It is impossible that any of the cells experienced temperatures during the 11-week storage greater than 80°F. We are unable to account properly for these observations*: (1) that recovery of damage occurs in p-type silicon (and perhaps in n-type silicon) at room temperature, and (2) that simultaneously the annealing kinetics of Bemski and Augustyniak[2] are obeyed. Further investigation can be expected to clarify these apparently conflicting observations.

The spectral response of the p on n solar cells degrade similar to the results obtained in the 740 Mev experiment, Figure 16. The spectral response characteristics of the n on p cells, due to a shallower diffused junction, contained slightly more short wavelength response than did the p on n cells with diffused junctions of the order of one to two microns below the surface. A typical spectral response character-

*Similar observations have been made also by W. L. Brown of BTL (private communication).

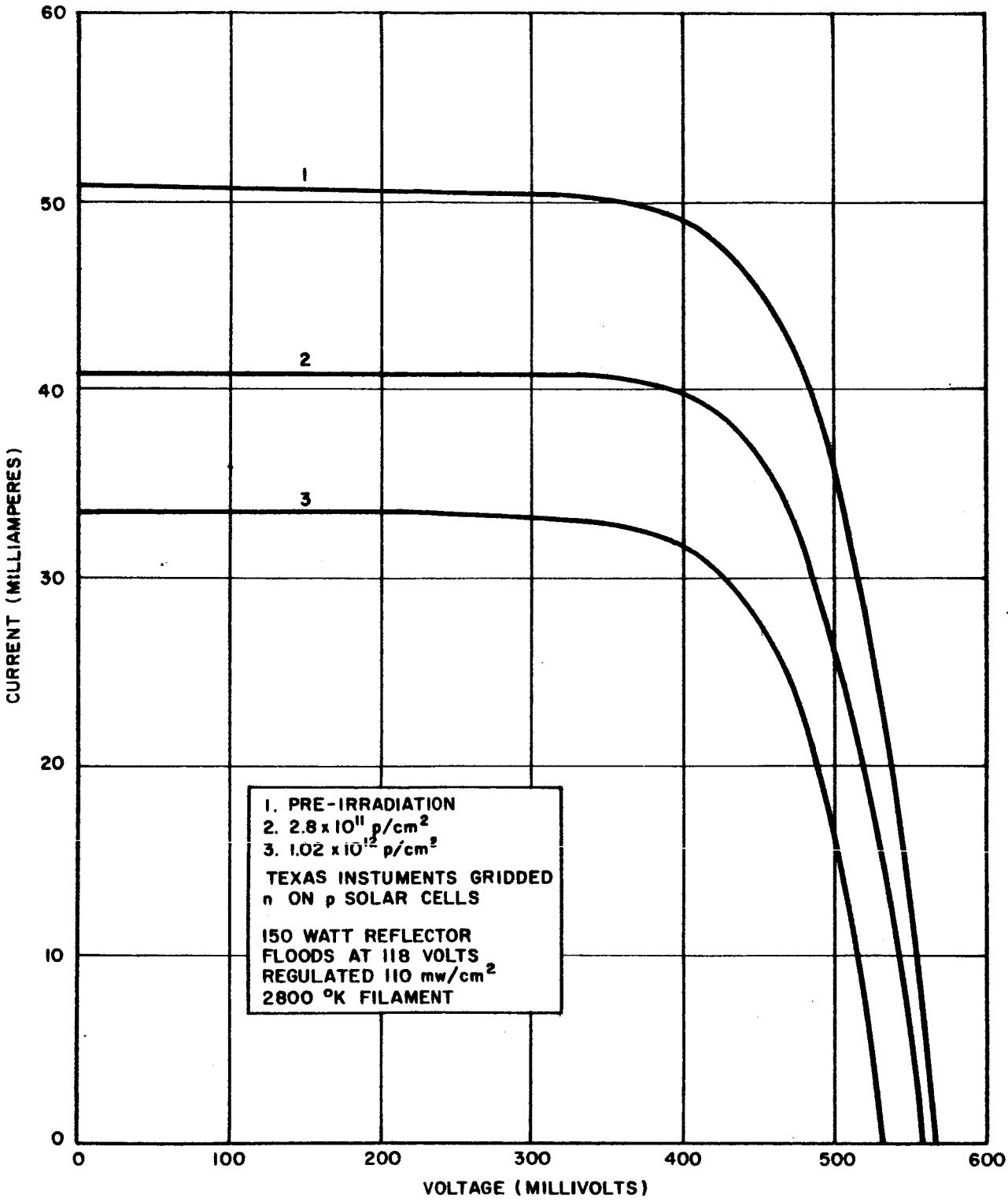

Figure 14. Texas Instruments N on P Gridded Silicon Solar Cell I-V Characteristic Degradation With 450 Mev Protons

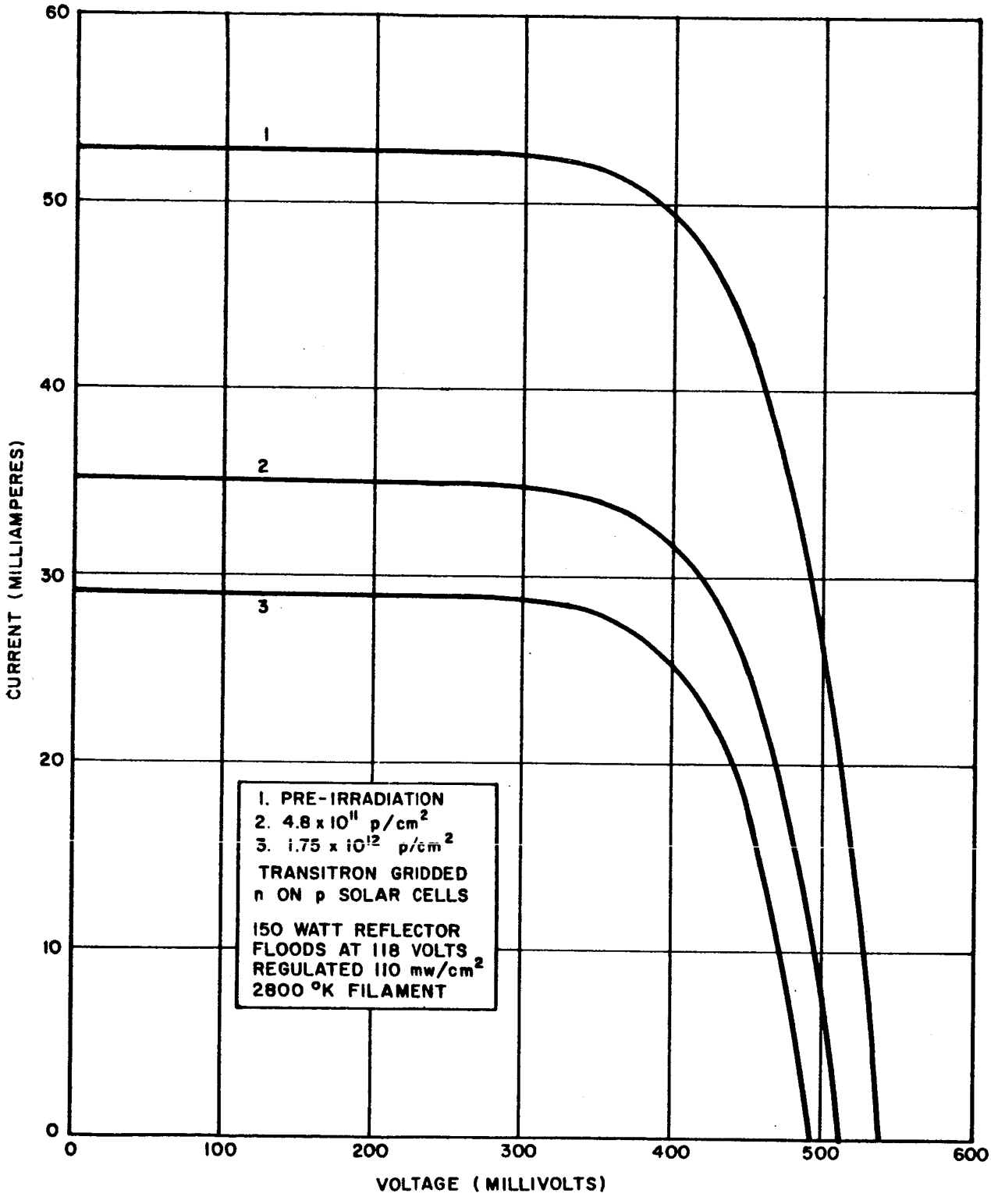

Figure 15. Transitron N on P Gridded Silicon Solar Cell I-V Characteristic Degradation With 450 Mev Protons

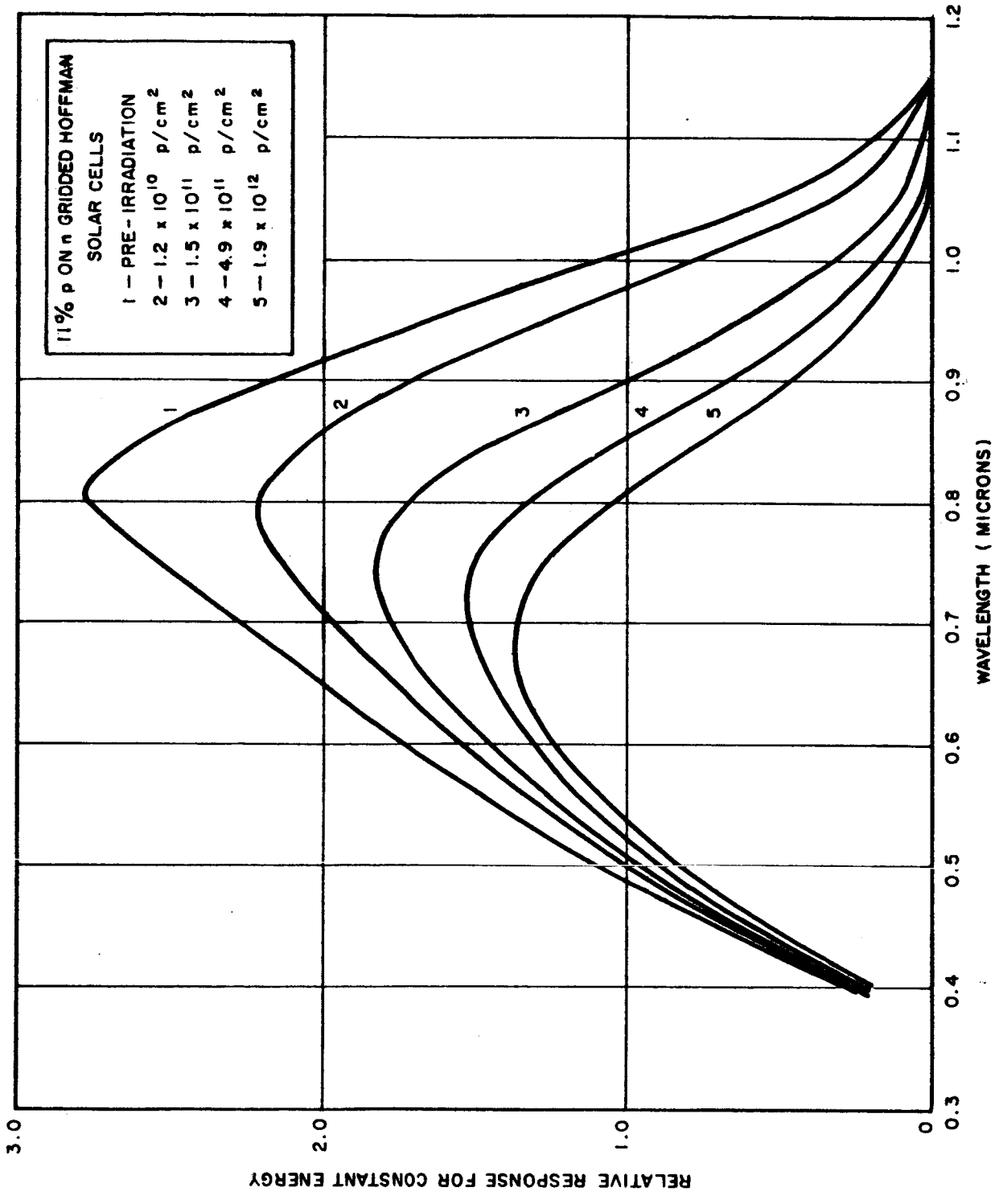

Figure 16. P on N Gridded Silicon Solar Cell Spectral Response Degradation With 450 Mev Protons

istic for a shallow diffused junction n on p silicon solar cell is shown in Figure 17. Two curves are shown in the figure, one for constant energy per wavelength interval, the other for constant photon flux per wavelength interval. The latter curve exhibits a region of uniform response versus wavelength which is expected under the assumption of unit quantum efficiency and minority carrier diffusion lengths in the surface layer which are of the order of the surface layer thickness. Although most of the n on p solar cell specimens were not obtained in sufficient time to acquire a complete set of preirradiation spectral response characteristics, several cells were examined and the results were no different than previously illustrated. Due to the higher short wavelength component produced by the shallow diffused junction, however, the rate of short circuit current degradation under either sun or tungsten illumination will appear to be less than that of the deeper diffused junction solar cells. Figure 18 illustrates a typical spectral response characteristic for gallium arsenide cells of the type irradiated in this experiment. As in the previous case, curves for both constant energy and constant photon flux are illustrated.

3.3 20.5 Mev Experiments

The 20.5 Mev experiments at UCLA were conducted in order to verify data previously obtained at low proton energies[3]. These experiments provided the opportunity for conducting a wider variety of investigations than previously attempted at higher energies. Previous experience at 740 Mev and 450 Mev had demonstrated that selection of experimental cells provides good experimental reproducibility and suggested that future experiments could rely upon cell selection rather than extensive statistics. Consequently, a wider variety of cells was chosen with the objective of comparing parent material and cell geometry with radiation damage rates. The results of the UCLA experiments are summarized in Figure 19.

The standard p on n ungridded solar cells, Figure 19, exhibit 25 per cent reduction in short circuit current at an integrated proton flux of 4×10^{10} p/cm^2. This result is in good agreement with a previously reported value (Loferski and Rappaport) at 17.6 Mev. The standard

---

[3] J. J. Loferski and P. Rappaport, RCA Review, 19, 563, (1958)

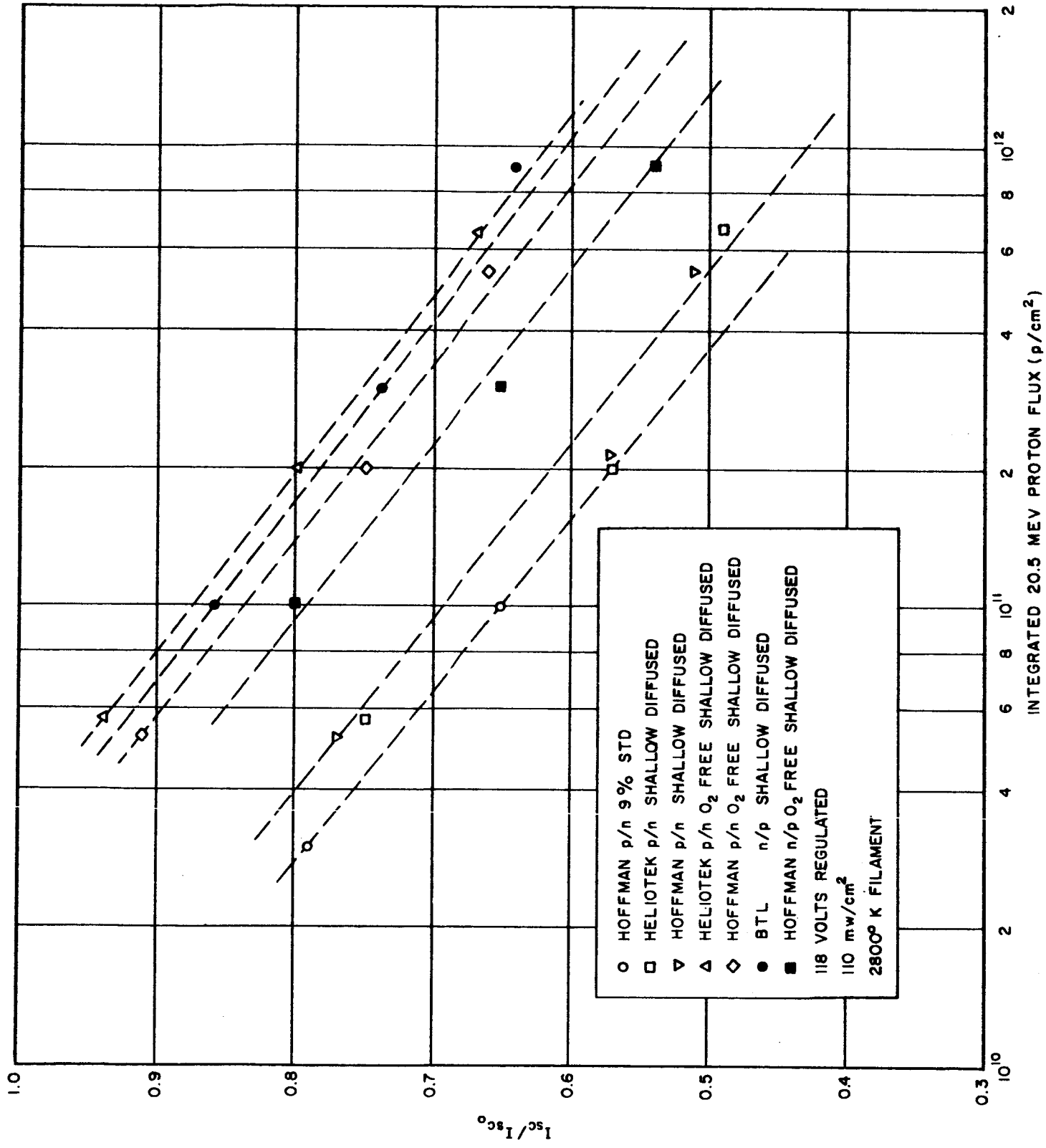

Figure 19. Silicon Solar Cell Short Circuit Current Degradation With 20.5 Mev Protons

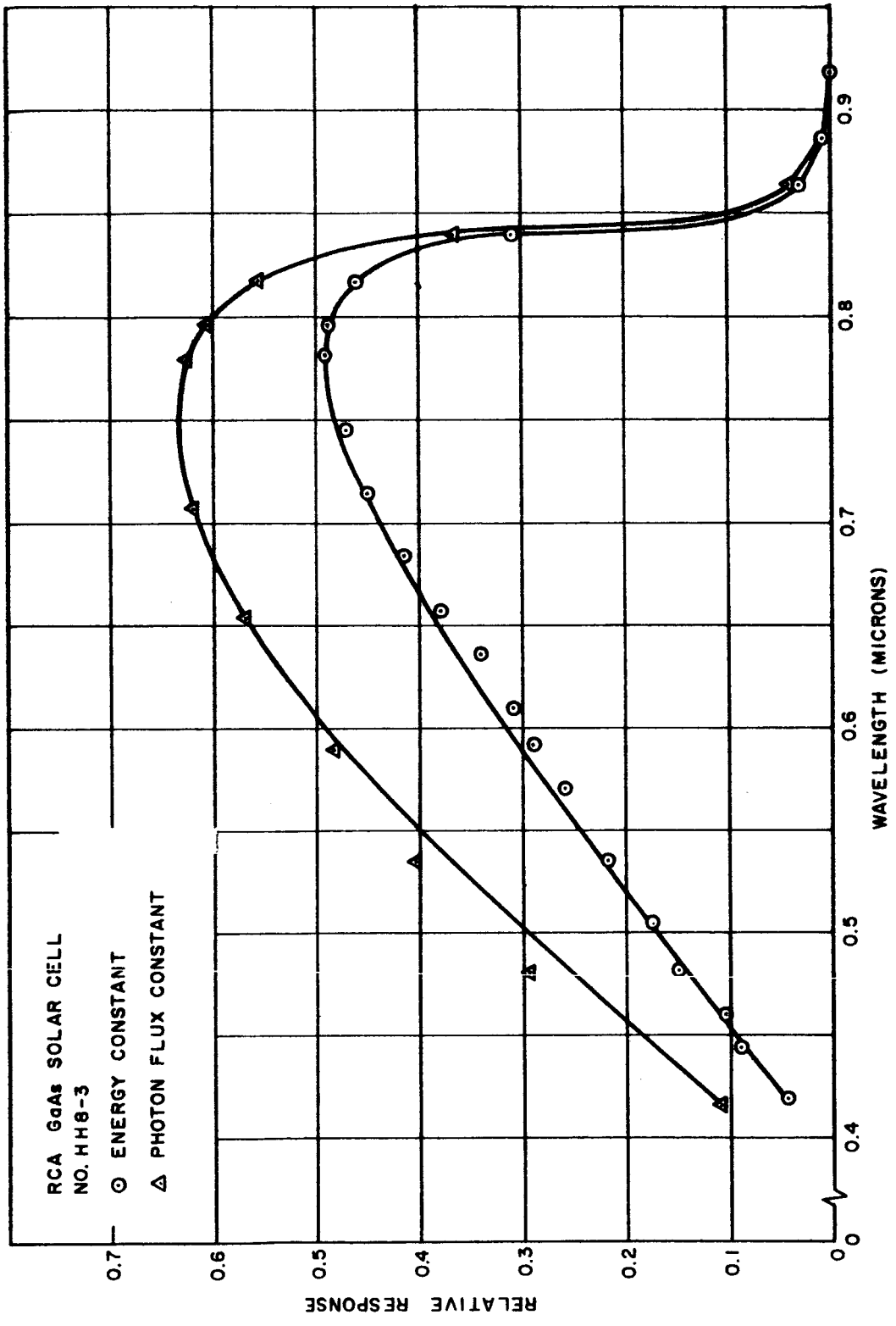

Figure 18. Typical Gallium Arsenide Solar Cell Spectral Response Curve

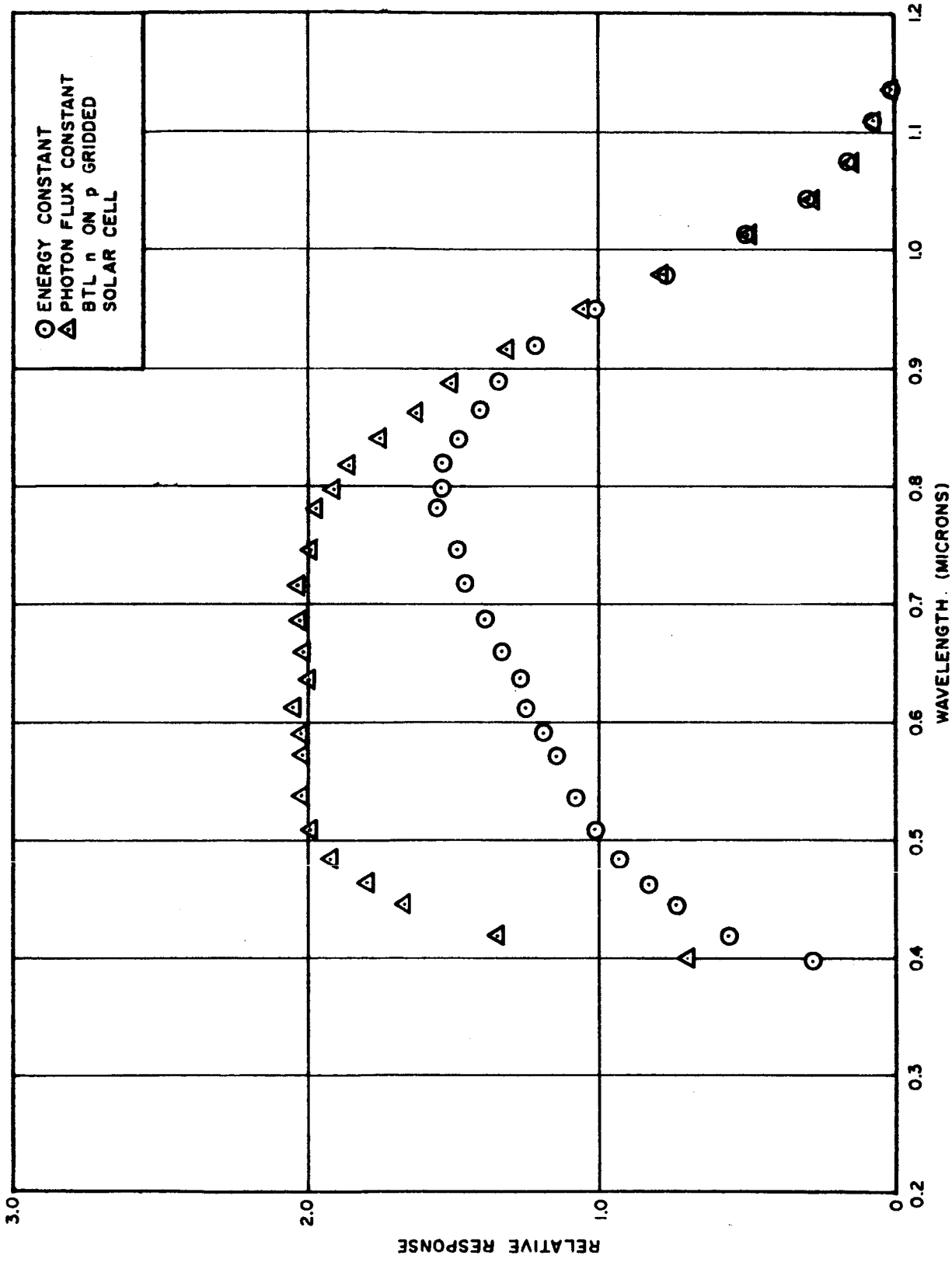

Figure 17. Typical N on P Shallow Diffused Silicon Solar Cell Spectral Response Curve

9 per cent ungridded cells are probably very similar to the cells used by Loferski and Rappaport in their earlier experiments and, for this reason, are the cells chosen for comparison. The rate of change of short circuit current with the log of the integrated proton flux at 20.5 Mev is the same as observed in the 740 Mev and 450 Mev experiments. Figure 19 shows that a 25 per cent change in short circuit current occurs for each decade of integrated proton flux under 2800°K illumination. Because of the nearly exponential optical dispersion in silicon, this degradation rate depends most strongly upon the spectral distribution of the illumination as observed earlier. The rate of change of short circuit current with log integrated flux, therefore, is independent of the proton energy providing that the same damage mechanism prevails at various energies. Comparison of Figures 5, 12, and 19 demonstrates this fact, confirming the expectation that proton irradiation produces reduction in minority carrier lifetime and minority carrier diffusion length through creation of point defects or clusters of defects.

The amount of damage which occurs is dependent upon both the proton integrated flux and the type of cell as shown in Figure 19. Under white light, these damage curves are characterized by the point at which damage begins. The "knee" of the curve (e.g., Figure 12) is one way of characterizing this damage. Figure 19 shows the dependence of the onset of damage to a variety of solar cell parameters, and comparison with the results obtained at 740 Mev and 450 Mev discloses the effect of change of proton energy on this "knee". It is also convenient to compare the response of selected solar cells on the basis of the point at which they suffer 25 per cent loss of short circuit current. These data have been referred to in discussing other figures in this report.

Spectral response curves and current-voltage characteristics for all the solar cells represented in Figure 19 were obtained before and after irradiation. These data are not presented because they are identical with the results obtained at similar degradations at 450 Mev and 740 Mev. For a given solar cell type, the change in current-voltage characteristic is independent of the proton energy producing the change; that is, the characteristic at a given temperature for a given change in short circuit current is independent of the method by which the change was generated. Spectral response and current-voltage characteristics

for cells shown in Figure 19 can be accomplished by referring to earlier figures of spectral response and current-voltage characteristics in this report, modifying those characteristics according to the proton flux indicated in Figure 19.

All of the cells shown in Figure 19 are shallow diffused with the exception of the 9 per cent p on n "standard". These cells have been selected as representative of parent material and cell geometry and are not selected in order to show preference for a particular manufacturer. However, the manufacturing source of the cells shown in Figure 19 is indicated. It is interesting to note that the variation in parent solar cell material and cell geometry controls the radiation response over a wide range. The data in Figure 19 span a factor of 10 in proton flux for the same degradation in short circuit current. Comparison of all cells irradiated, in addition to those shown in Figure 19, indicates that this dependence spans at least a factor of 20 in proton flux for the same degradation. This spread does not necessarily indicate the limits obtainable, because a limited number of variables have been investigated.

The two lower curves in Figure 19 demonstrate the importance of cell geometry. The materials used in these solar cells are very similar. The diffusion techniques differed only to the extent of the diffusion of boron into the parent n-type silicon. The standard 9 per cent cell has a geometrical junction one to two microns below the upper surface, whereas, the shallow diffused cells have a junction about $\frac{1}{2}$ micron below the upper surface. The data in Figure 19 suggest that the difference in radiation sensitivity may be about a factor of two between shallow diffused and deep diffused cells from similar parent material. Obviously, in order to avoid prohibitive series resistance, the shallow diffused cells require gridding of the upper surface. As mentioned earlier, this gridding has no effect on the radiation sensitivity of the cell. Because of the optical dispersion, minority carriers are generated by blue light near the cell surface. Red light generates carriers uniformly and deeply in silicon. Only the carriers generated within a diffusion length of the junction are collected. The boron doped surface layer has a very short diffusion length ($< 1\mu$) because of the high boron concentration. Therefore, the shallow diffused cells

have a higher collection efficiency for blue light generated carriers. Irradiation reduces the minority carrier diffusion length below the junction in the bulk silicon where the red light generated carriers predominate. This reduction in red response is the same in both shallow and deep diffused cells; however, shallow diffused cells, having a higher blue response, appear less sensitive to proton bombardment under white light.

The comparative superiority of n on p cells over p on n cells is also found at 20.5 Mev. Figure 19 shows approximately the same improved radiation resistance of n on p cells over conventional p on n cells as observed at 450 and 740 Mev. For comparison, normalized short circuit current is plotted; the initial efficiency of the p on n cells exceeded the efficiency of the n on p cells.

Previous experiments[4,5] on heavily damaged n-type silicon demonstrated the importance of oxygen in controlling some aspects of electron radiation effects. In an effort to investigate the relation between oxygen and radiation damage in silicon solar cells, a variety of cells was prepared from oxygen-free silicon. The silicon used in all these cells was prepared by the float zone process and had similar initial resistivities. The effect of geometry was eliminated as far as possible by conducting shallow diffusions ($\frac{1}{2}$ micron) for both the p on n and n on p cells. Supporting the earlier observations on heavily damaged silicon, Figure 19 shows the drastic improvement in radiation resistance of p on n cells produced from oxygen-free float zone silicon. Of special interest, however, is the observation that the performance of n on p cells deteriorates upon preparation with oxygen-free silicon. The use of oxygen-free silicon in the production of p on n cells results in an improvement of radiation resistance, according to the data in Figure 19, of about a factor of five. The oxygen-free p on n cells which describe the upper curve in Figure 19 are the most radiation resistant solar cells which have been observed in the course of all experiments. Their performance exceeds that of any n on p cells which have been investigated. P on n cells generally exhibit, for carefully prepared cells, higher efficiencies than observed

---

[4] G. Bemski, Journal Applied Physics, Vol. 30, No. 8, 1195, (1959)

[5] G. D. Watkins, J. W. Corbett, and R. M. Walker, Journal Applied Physics, Vol. 30, No. 8, 1198, (1959)

for n on p cells. The improved radiation resistance of p on n cells coupled with a higher efficiency suggests, at the present, considerable performance margin.

The preparation of n on p cells from oxygen-free silicon appears to deteriorate their radiation resistance. Figure 19 suggests the oxygen-free n on p cells are about a factor of two more sensitive to proton bombardment than n on p cells prepared from solar grade silicon. Obviously, extensive investigation of this observation has not been performed. Initial resistivities and cell geometries were nearly identical in the comparative cases in Figure 19.

Obviously, there are a number of difficulties in interpreting the data summarized in Figure 19. The oxygen concentration in float zone silicon is generally agreed to be 10^{15} oxygen atoms per cubic centimeter. The oxygen concentration in grown crystals is about $10^{18}/cm^3$. In these lightly damaged specimens, the defect concentration is probably about $5 \times 10^{13}/cm^3$ for 25 per cent reduction in short circuit current. If these considerations obtain, the oxygen concentration in even the oxygen-free silicon is 100 times the defect concentration. This circumstance is in contrast to the experiments conducted by Watkins, et al, in which the defect concentration was of the order of 10^{16} to $10^{17}/cm^3$. In these solar cell experiments, it is difficult to understand how the change in oxygen concentration from 10^5 times the defect density down to 10^2 times the defect density can control the production of trapping and recombination centers sufficiently violently to produce the large change observed in radiation resistance. If, as Watkins suggested, the oxygen combines with a point defect to produce an electrically important center, the oxygen concentration in even the float zone silicon should be sufficiently abundant to avoid an oxygen limited trap center production. We are unable, at present, to account for the observations shown in Figure 19 related to the improved radiation resistance of oxygen-free p on n solar cells.

Similarly, if one accepts the observations on p on n cells, it is difficult to interpret the effect of oxygen-free silicon on the radiation sensitivity of n on p solar cells. The argument might proceed similar to the discussion for p on n cells. Even allowing in the

case of the p on n cells for the possibility of control of the production of trapping centers by oxygen, it is difficult to understand how the removal of oxygen can increase the rate of formation of trapping centers in n on p solar cells.

The comparison of float zone silicon and grown silicon crystals with respect to oxygen concentration does not account for the difference in dislocation density in the two materials. Grown silicon crystals customarily have low dislocation concentrations, whereas, float zone silicon is characterized by high dislocation densities. The observations summarized in Figure 19 may be interpretable in terms of the dislocation densities in contrast to the oxygen concentration. Evidently, investigation of this point requires preparation of oxygen-free low dislocation density silicon crystals and oxygen-rich high dislocation density crystals for further comparison. However, for the present, there seems to be no simple explanation of the observations summarized in Figure 19.

4.0 CONCLUSIONS

The experimental results presented in this report emphasize the radiation sensitivity of solar cells. Because solar cells require long minority carrier diffusion lengths for efficient operation, they are probably more radiation sensitive than most semiconductor devices. The radiation sensitivity depends upon a number of factors, including proton energy, light spectrum, cell type, cell geometry, and parent material characteristics. It is difficult to generalize the relationship of these factors; however, mindful of the need to provide design data, Figure 20 has been prepared. A spread in damage sensitivity for both tungsten and sun illumination is shown. Average values for shallow diffused p on n cells are shown at the bottom of the response "bands" in Figure 20. Upper limits of radiation resistance comprise the oxygen-free p on n cells, and n on p cells should respond near the upper limit of radiation resistance. An individual cell, depending on many factors, can be expected to respond according to a curve within the band, but it must be emphasized the band does not represent a statistical sampling. Commercial p on n cells may lie at the bottom of, or below, the band.

Comparison of the experimental results at a number of proton energies shows that the rate of degradation of short circuit current with the log of the integrated proton flux is a constant. This is shown, for example, in Figure 20. The rate of change with the log integrated flux is independent of the proton energy at least in the range 20 Mev to 740 Mev. Under sunlight, this rate is about 15 to 20 per cent degradation per decade of integrated flux. The onset of radiation damage, i.e., the "knee", tends to be insensitive to the spectrum of the light source. The rate, however, depends upon the spectral distribution.

The comparative advantages of other cell materials, for example gallium arsenide, have not been conclusively investigated in these experiments. However, it is important to consider the effect of absolute cell efficiency with the rate of radiation damage. Cells of low initial efficiency, including gallium arsenide, may not possess any real advantage over higher efficiency cells which begin to exhibit radiation damage at lower integrated fluxes.

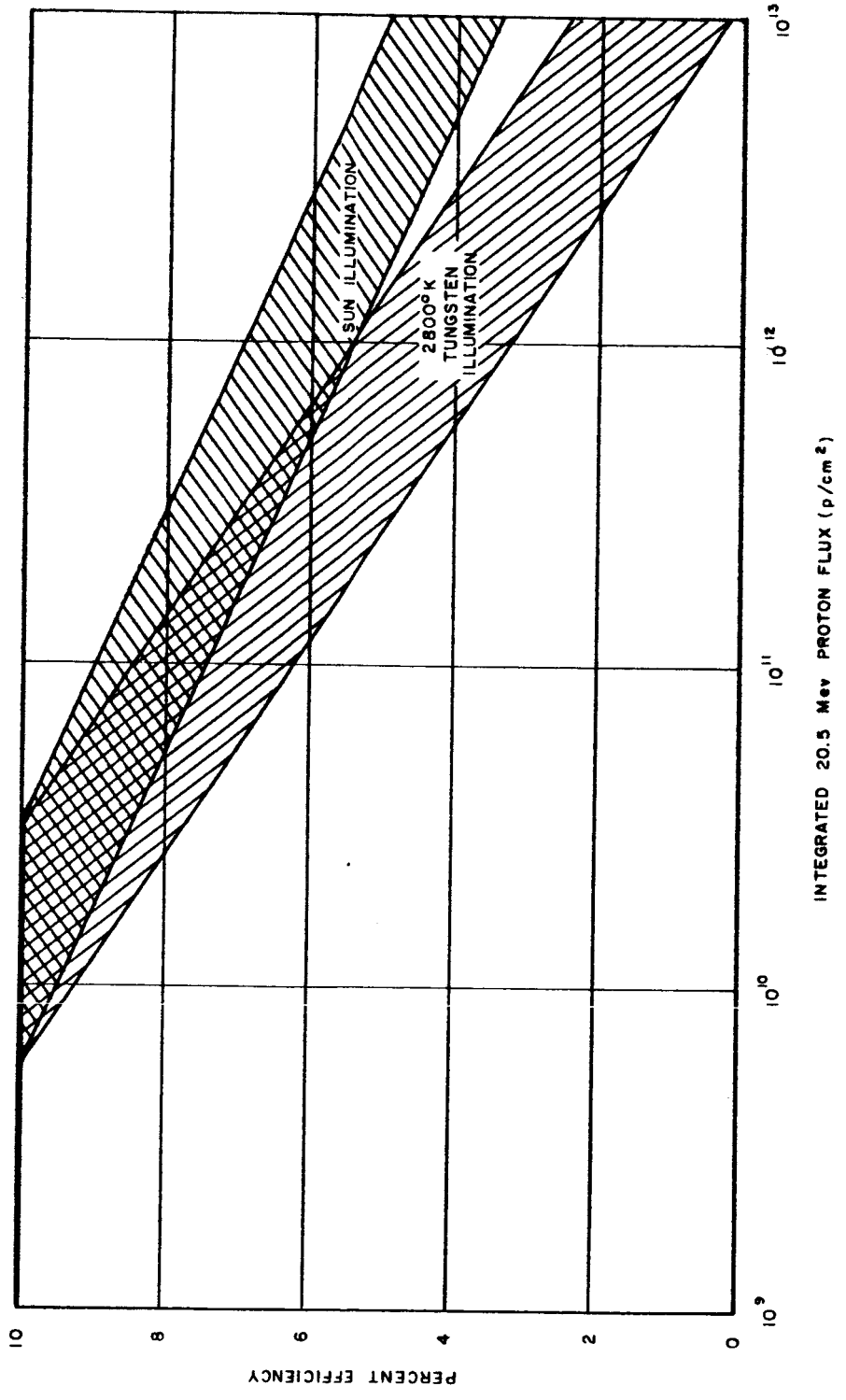

Figure 20. Typical Silicon Solar Cell Power Output Degradation During Proton Bombardment

Shallow diffused p on n solar cells produced from oxygen-free silicon exhibit the highest degree of radiation resistance found in any silicon solar cell. The oxygen-free p on n cells exceed in this regard n on p silicon solar cells. This increased radiation resistance coupled with the higher initial efficiency of p on n cells suggests a clear-cut advantage to oxygen-free p on n cells at the present time. It has been pointed out, however, that the presence of oxygen may not be the controlling factor in producing the increased radiation resistance. Preliminary analysis suggests that oxygen may not be responsible and some other defect or impurity may be the controlling variable. Such an impurity has not yet been identified.

In many spacecraft applications, because the accrual of damage occurs slowly, the possibility of annealing at near normal operating temperatures is an attractive one. Evidence of annealing in some silicon solar cells, particularly the n on p, suggests this factor as a possible future consideration. In particular, this advantage argues against the p on n cell and in favor of the n on p cell, providing the mechanism can be identified and used to its fullest advantage.

The development of silicon solar cells with increased radiation resistance requires a detailed understanding of the mechanism of defect production in silicon as suggested by these experiments. Increased performance can be expected as a result of future research.